Am J Cancer Res 2022;12(8):3679-3692
www.ajcr.us /ISSN:2156-6976/ajcr0143986

Original Article

Nicotine dose-dependent epigenomic-wide DNA methylation changes in the mice with long-term electronic cigarette exposure

Gang Peng[1*], Yibo Xi[2*], Chiara Bellini[3], Kien Pham[2], Zhen W Zhuang[4], Qin Yan[2], Man Jia[2], Guilin Wang[5], Lingeng Lu[6], Moon-Shong Tang[7], Hongyu Zhao[1], He Wang[2]

[1]Department of Biostatistics, Yale University School of Public Health, New Haven, USA; [2]Department of Pathology, Yale University School of Medicine, New Haven, USA; [3]Department of Bioengineering, College of Engineering, Northeastern University, USA; [4]Department of Cardiovascular Medicine, Yale University School of Medicine, New Haven, USA; [5]Department of Genetics, Yale University School of Medicine, New Haven, USA; [6]Department of Chronic Disease Epidemiology, Yale University School of Public Health, New Haven, USA; [7]Department of Environmental Medicine, New York University School of Medicine, New York, USA. [*]Equal contributors.

Received May 7, 2022; Accepted June 16, 2022; Epub August 15, 2022; Published August 30, 2022

Abstract: Epigenomic-wide DNA methylation profiling holds the potential to reflect both electronic cigarette exposure-associated risks and individual poor health outcomes. However, a systemic study in animals or humans is still lacking. Using the Infinium Mouse Methylation BeadChip, we examined the DNA methylation status of white blood cells in male ApoE-/- mice after 14 weeks of electronic cigarette exposure with the InExpose system (2 hr/day, 5 days/week, 50% PG and 50% VG) with low (6 mg/ml) and high (36 mg/ml) nicotine concentrations. Our results indicate that electronic cigarette aerosol inhalation induces significant alteration of 8,985 CpGs in a dose-dependent manner (FDR<0.05); 7,389 (82.2%) of the CpG sites are annotated with known genes. Among the top 6 significant CpG sites (*P*-value<1e-8), 4 CpG sites are located in the known genes, and most (3/5) of these genes have been related to cigarette smoking. The other two CpGs are close to/associated with the *Phc2* gene that was recently linked to smoking in a transcriptome-wide associations study. Furthermore, the gene set enrichment analysis highlights the activation of MAPK and 4 cardiomyocyte/cardiomyopathy-related signaling pathways (including adrenergic signaling in cardiomyocytes and arrhythmogenic right ventricular cardiomyopathy) following repeated electronic cigarette use. The MAPK pathway activation correlates well with our finding of increased cytokine mRNA expression after electronic cigarette exposure in the same batch of mice. Interestingly, two pathways related to mitochondrial activities, namely mitochondrial gene expression and mitochondrial translation, are also activated after electronic cigarette exposure. Elucidating the relationship between these pathways and the increased circulating mitochondrial DNA observed here will provide further insight into the cell-damaging effects of prolonged inhalation of e-cigarette aerosols.

Keywords: Electronic cigarette, epigenomic-wide DNA methylation, dose-dependent, MAPK signaling pathway

Introduction

Introduced into the USA market in 2007 [1] as a healthy alternative to conventional cigarettes, e-cigarettes have experienced widespread acceptance among smokers, non-smokers, and especially the youth ever since [2]. The long-term health effects of e-cigarettes in humans are far from clear, and the causal inference study of e-cigarette user-health outcomes is time-consuming and costly. As an intermediate surrogate marker, DNA methylation does not change nucleotide sequences but partially determines chromatin structure and patterns of gene expression [3]. Results from traditional smoking and pilot studies of e-cigarette vaping suggest that the alteration of DNA methylation has the potential to reflect smoking/vaporing exposure and predict health effects, making it an ideal health biomarker of vaporing [4, 5].

It has been well established that traditional cigarette smoking modulates DNA methylation in many CpG sites in an exposure concentration- and timing-dependent manner, suggesting that DNA methylation is induced not only by the

exposure itself but also by the chemical concentration within the products [6-9]. The Epigenetic Smoking status Estimator, EpiSmokEr, is recently developed as a smoking status prediction tool by analyzing the DNA methylation pattern of peripheral blood cells with a machine learning algorithm (multinomial LASSO regression) [10]. In contrast to the extensive literature on cigarette-induced DNA methylation alteration, the study on e-cigarette-induced alteration of DNA methylation is in its early stage [11]. Using DNA from bronchial brushing samples of 32 subjects, Song et al. identified 451 differentially methylated CpGs at a false discovery rate (FDR) $q<0.1$; but in 97% of the CpGs methylation levels, e-cigarette users are between smokers and never-smokers [12]. Using leukocyte genomic DNA from 45 subjects, Caliri et al. showed that e-cigarette users and cigarette smokers have significant loss of methylation in LINE1 retroelements compared to controls [4]. These pilot studies clearly suggest that e-cigarette alters DNA methylation status; however, the small sample size and the limited number of DNA sequences analyzed make their results less conclusive or inclusive.

Extensive investigations in the last decade have suggested that DNA methylation signature is one of the determinant factors for human health, as methylation pattern partially shapes gene expression and sets up phenotypes, including potential initiation/progression of diseases and all-cause mortality [5]. In several common disorders, DNA methylation appears to explain a more significant portion of the measurable variance in complex traits than genetics [13, 14]. In a study using 13 clinical traits in adipose tissue, methylation of the fatty acid synthase locus alone could account for 16% of BMI variation [15]. For comparison, 97 genetic variants identified in a large genome-wide association study explain merely 2.7% of the BMI variance [16]. Given the established critical role of genome-wide DNA methylation signature as a biomarker of cigarette smoking-induced health effects and exposure status predicator, we propose that genome-wide DNA methylation will also serve as a potential biomarker for e-cigarette vaping-induced systematic health effects and exposure status.

In the current study, ApoE-/- mice were divided into 3 groups based on different concentrations of nicotine in e-cigarettes (0, 6 mg/ml, and 36 mg/ml) and exposed for 14 weeks. Methylation of DNA from circulating white blood cells was profiled with Infinium Mouse Methylation BeadChip Kit, interrogated over 285,000 methylated CpGs in the promoters, gene bodies, and enhancer regions for genome-wide methylation at single-nucleotide resolution. Our results indicate e-cigarette induces extensive, dose-related alteration in the methylation pattern of DNA.

Material and methods

Animal use

5-week-old ApoE-/- mice were purchased from Jackson Laboratories (Bar Harbor, ME). All procedures were carried out following a protocol approved by Yale University Institutional Animal Care& Use Committee (IACUC).

E-cigarette exposure

In a series of experiments, mice were exposed to E-Cig vapor using the InExpose system specifically customized by Scientific Respiratory Equipment Inc. (Canada) for 2 hours/day, 5 days/week, for 14 weeks. The E-Cig formula (6 mg/ml or 36 mg/ml nicotine dissolved in 50% PG and 50% VG) and exposure setting were optimized according to the American E-Cig Liquid Manufacturing Standard and American Vaping Standard. Sixteen mice per group were subjected to whole-body exposure, while the control mice were exposed to HEPA filtered room air. At the experimental endpoint (12 hours after the last exposure), all mice were euthanized with CO_2, followed by cervical dislocation. 500 µl of whole blood from each mouse was collected from vena cava, mixed with 50 µl of 1 unit/µl Heparin (H3393, Sigma), and subjected to flow cytometry for white blood cell sorting and to DNA extraction for epigenetic analysis.

Cotinine measurement

Successful intake of e-cigarettes after exposure was confirmed by mouse cotinine tests. The urine collection was done during the experimental endpoints and within 1 hour after the last E-Cig exposure. A mouse/Rat Cotinine ELISA kit (CO096D-100, Calbiotech Inc.) was used to measure the cotinine level, following

the protocol supplied by the kit. All tests were performed at room temperature and read absorbance on the microplate reader at 450 nm within 15 minutes after adding the stopping buffer. The standard curve was used to quantify cotinine concentration in the tested samples.

Flow cytometry with whole blood samples

100 μl of anticoagulant-treated whole blood collected from animals at the experimental endpoint was subjected to red blood cell lysis, according to the manufacturer's protocol. After red blood cell lysis, the remaining cells were stained with 4 fluorochrome-conjugated anti-mouse antibodies and analyzed on a FACSCanto LSRII flow cytometer (BD Biosciences). The antibody panel was designed based on various criteria, such as fluorochrome brightness, antigen density, co-expression, fluorochrome spillover of interested immune-cell subsets, and reagent availability in each panel for the available flow cytometer. Isotype controls were used to set the appropriate gate. Data were acquired with FACSDiva and analyzed with FlowJo 6.4.7v10.6. Approximately 20,000 cells were used to generate a scatter plot for each sample.

Blood cell DNA extraction, processing, and methylation profiling

Anticoagulant-treated mouse blood was centrifuged at 3500 rpm for 15 minutes to isolate the white blood cells and plasma. Both white blood cells and plasma were stored at -80°C for future tests. The Qiagen DNeasy Blood & Tissue kit (69506, Qiagen) was used for DNA extraction from the white blood cells. The extracted DNA was quantitated with a Qubit quantification assay (Thermo Fisher Scientific, Ecublens, Switzerland). Bisulfite-converted DNA was amplified and hybridized with Infinium Mouse Methylation BeadChip, including >285,000 markers (Illumina, CA, USA), and then scanned with Illumina iScan system (Illumina, CA, USA), following the manufacturer's protocols.

Preprocessing of methylation data

DNA methylation data were preprocessed with the R package 'Enmix' [17]. Methylation data were first corrected for dye bias with the RELIC method [18] and then were quantile normalized. For quality control (QC), the samples with more than 5% of all CpG sites with a detection *P*-value larger than 0.01 and samples with mismatched sex between phenotype data and methylation data were removed. At the CpG level, CpG sites with a detection *P*-value larger than 0.01 in more than 5% of all samples (more than 1 sample in this study) were removed. Only CpG sites on autosomes were studied, and the CpG sites on sex chromosomes were removed in this study. Principal component analysis of all CpG sites that passed QC was used to find whether there were any outliers or clusters in the samples.

Identification of CpG sites with methylation changing according to e-cigarette exposure dose

A linear regression model listed below was used to discover CpG sites in which the methylation level changes with e-cigarette exposure dose. There are 3 levels of dosage, namely 0, 6, and 36 mg/ml.

$$M = \beta_0 + \beta_1 * Dose$$

M is the log2 ratio of methylation over unmethylation. We used the M value, which is more statistically valid than the Beta value, the proportion of methylation, for statistical analysis, Beta value, which has a more intuitive biological interpretation, for figure demonstration [19].

Besides dose-based analysis, we also used t-test after dichotomizing the data into two different pairs of groups: 0 mg/ml group vs. 6 mg/ml + 36 mg/ml group and 0 mg/ml + 6 mg/ml group vs. 36 mg/ml group.

Gene set enrichment analysis

To identify potential functions of the genes associated with significant CpG sites, we performed gene set enrichment analysis using the R package 'clusterProfiler' [20] on the gene sets in the Kyoto Encyclopedia of Genes and Genomes (KEGG) and Gene Ontology (GO). We first identified genes associated with any significant CpG sites as significant genes. Then we only focused on genes with significant CpG sites in their promoter region for the enrichment analysis.

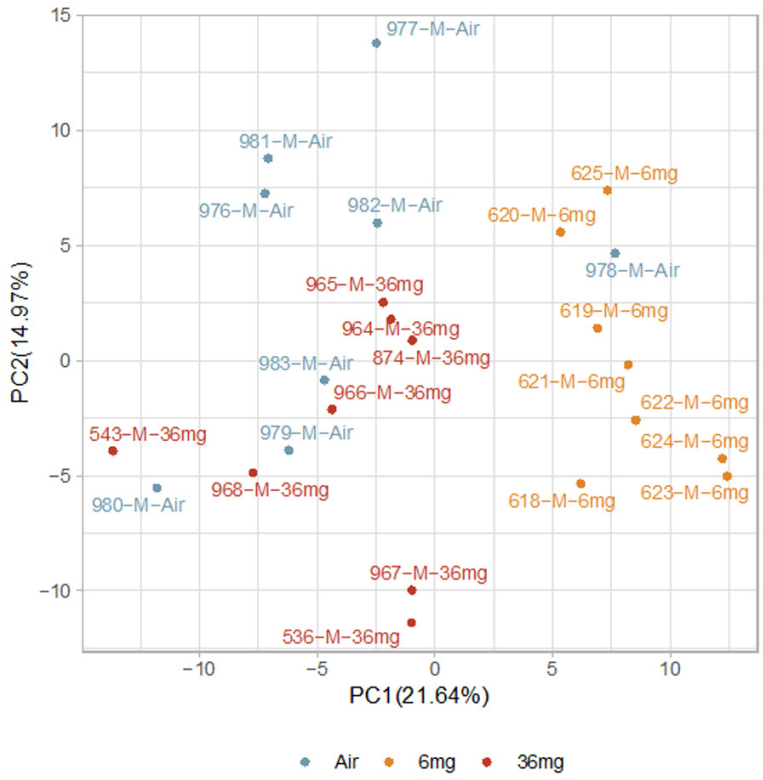

Figure 1. Scatter plot of the first two principal components of methylation data from all samples. The number in the parentheses is the proportion of variance.

Plasma cfDNA and mtDNA/nDNA ratio and oxidization of cell-free DNA

For measurement of *in vivo* plasma mtDNA/nDNA ratio, mice plasma was first subjected to cell-free DNA (cfDNA) extraction using Apostle minimax cfDNA extraction kit (ApostleBio, CA, US). Plasma cfDNAs were then used as templates for SYBR qPCR (Applied Biosystem, CA) with primers: murine 18S rDNA F: TAGAGGGACAAGTGGCGTTC; murine 18S rDNA R: CGCTGAGCCAGTCAGTGT; murine mtCO-1 F: GCCCCAGATATAGCATTCCC; murine mtCO-1 R: GTTCATCCTGTTCCTGCTCC. Amplification conditions were 95°C in 10 min; 95°C in 30 sec, 53°C in 30 sec for 40 cycles; followed by dissociation at 72°C in 30 sec, 95°C in 1 min, 55°C in 30 sec, and 95°C in 30 sec. The plasma mtDNA/nDNA ratio was calculated as the ratio of mtCO-1/18S rDNA. The relative fold-change of mtDNA was calculated using the 2-ΔΔCt method and compared to the control air group.

6.25 μl of a plasma sample from each mouse was used to do the DNA oxidization ELISA test using the DNA Damage Competitive ELISA Kit (EIADNAD, Invitrogen). 8-OHdG level in plasma can be used to indicate the DNA oxidization.

All data were collated using Microsoft Excel Software and analyzed using GraphPad Prism 5.0 (GraphPad, La Jolla, CA). All data are represented as the mean values, and error bars represent the mean's standard error (SEM). Samples in experimental cohorts were compared using Dunnett's multiple comparisons test. The difference was considered significant when $P< 0.05$.

Results

E-cigarette exposure and blood cell component

The rodent whole body E-cigarette exposure system adopted in our study has been widely used and reported [21, 22]. Successful and dose-dependent E-cigarette exposure was confirmed by measuring urine cotinine levels, which average at 0, 100, or 300,000 ng/ml for E-cigarette exposure with the nicotine dose at 0, 6, or 36 mg/ml, respectively (Figure S1). It is known that the DNA methylation in white blood cells could be influenced by the proportion of sub-compositions. A flow cytometry analysis of white blood cells showed that E-cigarette exposed mice had no significant change in the ratio of B lymphocytes, neutrophils, T lymphocytes, and monocytes when compared to air-exposed mice (Figure S2).

Preprocessing of methylation data

After removing CpGs with low quality and CpGs on chromosomes X and Y, there were 264,286 CpG sites left. Principal component analysis of the remaining CpG sites revealed differences among the three dose groups. The samples in each dose group were more likely to be clustered together. And we did not find any outliers from PCA (**Figure 1**). There were two peaks in

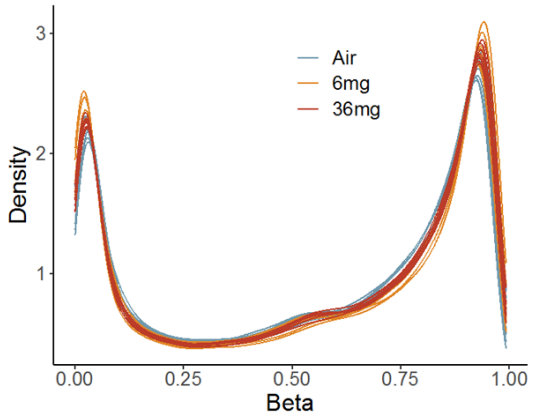

Figure 2. Beta value distribution of CpG sites on autosomes.

the Beta value distribution (**Figure 2**), similar to the human methylation profile [23] and consistent with the other mouse methylation study [24]. After QC, all samples were then subject to the following analyses.

CpG sites with methylation changing related to e-cigarette exposure dose

One unique design in the current study is the nicotine dose escalation, which is not easily evaluated in human e-cigarette vapers, as most studies are based on self-reported e-cigarette use. However, few human studies on traditional cigarette smokers have examined the potential nicotine dose-escalated effects on DNA methylation of white blood cells. We calculated the *P*-value for each CpG site in the regression model. A Manhattan plot of the CpG sites was shown in **Figure 3**. We observed 8,985 CpG sites that were significantly associated with e-cigarette exposure dose (FDR< 0.05, Table S1). Among them, 7,389 sites (82.2%) were annotated with known genes, and 2,492 sites (27.7%) were in the promoter regions of these genes (Transcription Start Site [TSS] 200, TSS1500). **Figure 4** shows the correlation between nicotine doses and methylation levels of the top 6 significant CpG sites (*P*-value<1e-8). Two of them were inversely associated with e-cigarette exposure dosages, while the other four were positively associated with e-cigarette exposure dosages. 4 CpG sites were located in the known genes (cg44389073: *Capns1*; cg34735002: *Znf598*; cg46803463: *Ccdc33* and *Stra6*; cg30601292: Tac4). *Capns1* was found differentially expressed in a subpopulation of airway perigoblet cells of smokers [25]. *Znf598* was among the top 50 smoking-dysregulated genes in human airway basal cells [26]. *Ccdc33* was also found to be influenced by smoking [27, 28]. Although not mapped to any known gene, cg41445486 was very close to *Phc2*, a risk gene linked to smoking [29], and miRNA expression changes in the smokers' spermatozoa [30]. *Phc2* was also associated with smoking in a transcriptome-wide associations study (http://twas-hub.org/traits/UKBB_SMOKING_STATUS/) [31]. Another CpG site, cg41446118, which is significantly associated with e-cigarette exposure in a dose-dependent manner (FDR=0.005), was also located in the gene body of *Phc2* (Table S1).

In the analyses of the data after dichotomization, we discovered 8,965 and 9,528 significant CpG sites for 0 mg/ml group vs. 6 mg/ml + 36 mg/ml group and 0 mg/ml + 6 mg/ml group vs. 36 mg/ml group, respectively (FDR< 0.05, Tables S2, S3). The overlaps of significant CpG sites from the 3 analyses can be found in Figure S3. 75.2% of significant CpG sites found in dose analysis are overlapped with the results from at least one of the dichotomized analyses. It is a validation of the dose analysis.

Significant gene sets associated with e-cigarette exposure dose

The studies from our group and others indicate that e-cigarette exposure resulted in systematic inflammation, as illustrated by increased cytokine expression. The recurring inflammation is partly triggered by TLR9 activation from elevated cytoplasmic and/or circulating mitochondrial DNA [32]. Electronic cigarette exposure significantly increased right ventricle free wall thickness at systole and diastole in C57BL/6 wild-type mice [33]. Recent evidence also showed that e-cigarettes decreased left fractional ventricular shortening and ejection fraction in a mouse model [34].

The gene set enrichment analysis with E-cigarette exposure was conducted using the R package 'clusterProfiler'. In the KEGG analysis, 33 gene pathways were enriched. The MAPK signaling pathways were at the top of the list and clearly related to the elevated cytokine expression after E-cigarette exposure. Four cardiomyocyte/cardiomyopathy-related pathways,

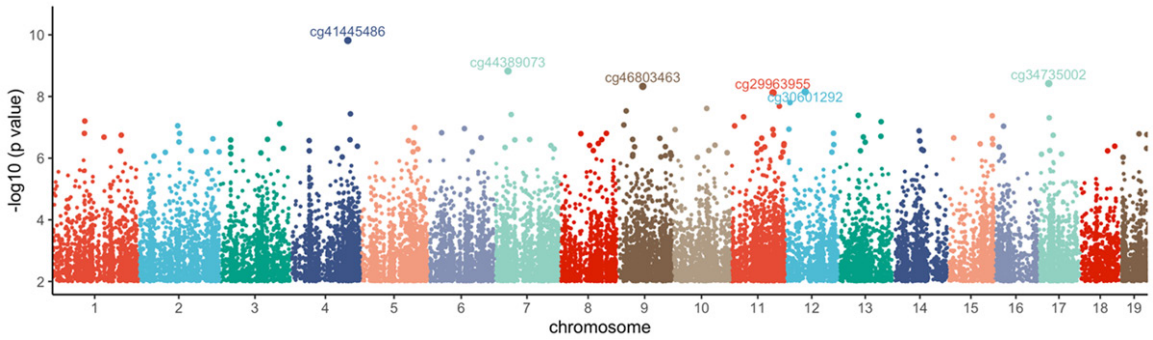

Figure 3. Manhattan plot of *P*-values for each CpG site on autosomes. CpG sites with a *P*-value larger than 0.01 are not included in the Figure.

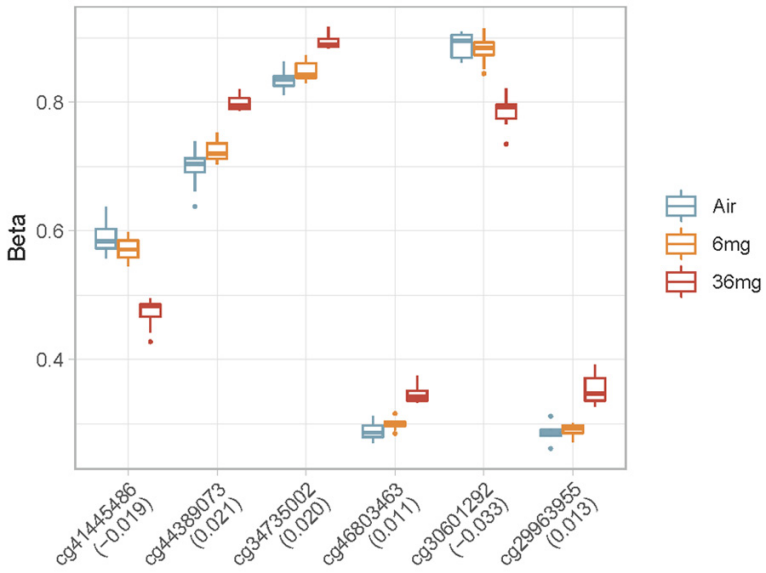

Figure 4. Boxplot of the Beta value of top 6 significant CpGs in 3 e-cigarette exposure dose groups.

including adrenergic signaling in cardiomyocytes, dilated cardiomyopathy, hypertrophic cardiomyopathy, and arrhythmogenic right ventricular cardiomyopathy, were also included in the top 10 gene pathway list (**Figure 5**, Table S4). The top 10 list from gene promoter analysis using GO highlighted two pathways related to mitochondrial activities: mitochondrial gene expression and mitochondrial translation (**Figure 6**, Table S5).

E-cigarette exposure results in increased mt/nDNA ratio and enhanced cfDNA oxidization

Circulating mitochondrial DNA is a pro-inflammatory damage-associated molecular pattern that triggers the formation of neutrophil extracellular traps in sickle cell disease [35]. It has been proposed as a biomarker for atrial fibrillation and coronary heart disease development in diabetic patients [36, 37]. Our study showed that long-term e-cigarette exposure induced an increased mtDNA/nDNA ratio in a nicotine dose-dependent manner (**Figure 7**), indicating that mitochondrial function has been affected after the E-cigarette exposure. The elevated mtDNA could be responsible for activating toll-like receptor 9 and resulted in cytokine mRNA expression in cultured monocyte and elevated plasma cytokine protein levels after e-cigarette exposure observed in our previous study [32]. Both cigarette smoking and e-cigarette vaporing have enhanced oxidative stress in cells and circulation [38]. In the current study, we illustrated that long-term e-cigarette exposure enhances oxidized cfDNA levels in a nicotine dose-dependent pattern (**Figure 8**).

Discussion

Most E-cigarette vaporing studies measure the exposure via self-report or nicotine metabolites such as cotinine levels. Self-reporting method is the most direct measurement of external vaporing, but it fails to measure the absorbed vapor. Although cotinine could serve as an internal dose of vaporing, it is only a short-term

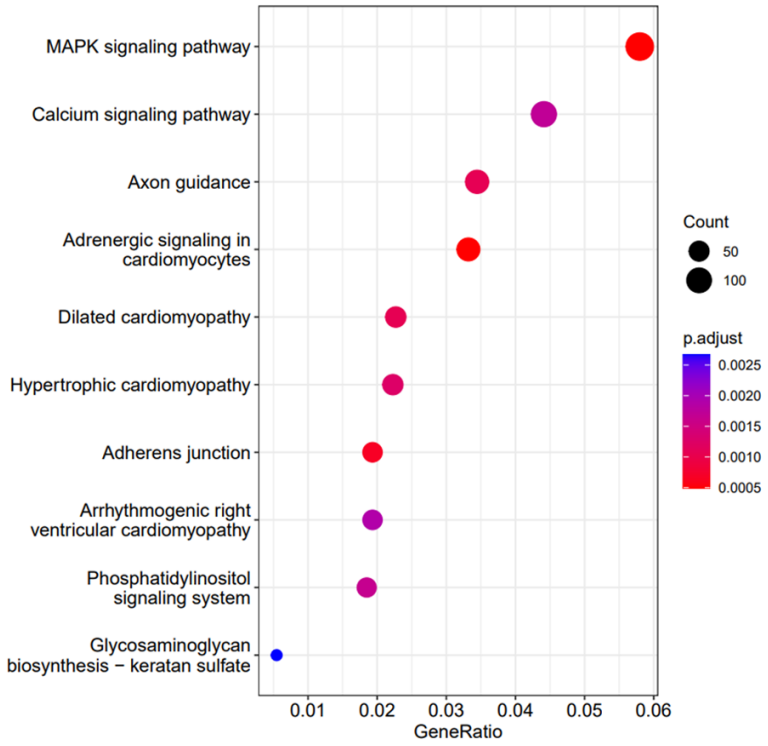

Figure 5. Top 10 significant KEGG pathways from enrichment analysis using genes associated with any considerable CpG sites (significant genes). Count: number of genes associated with any significant CpG sites in the pathway. GeneRatio: the ratio between the number of significant genes in a pathway and the number of significant genes in all KEGG pathways.

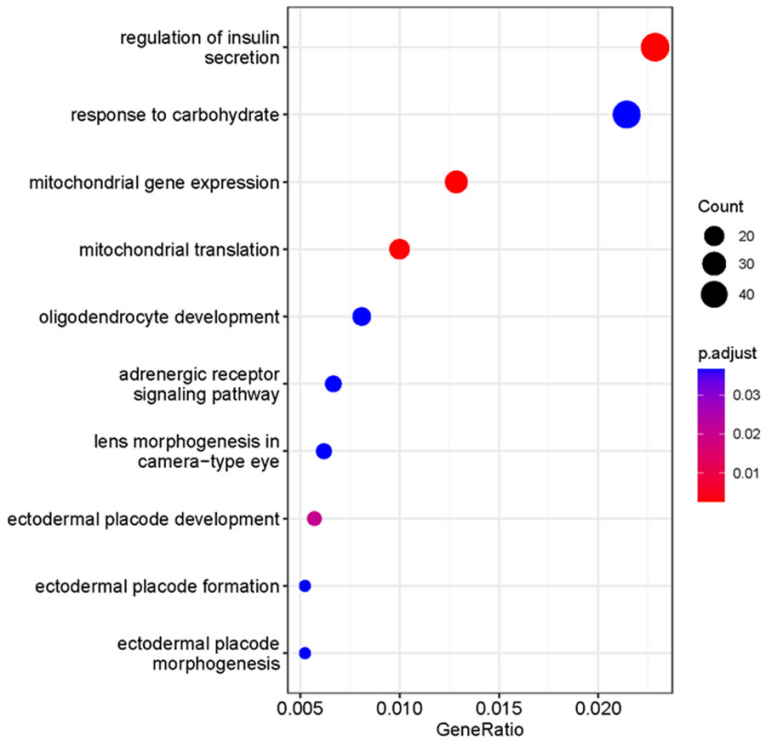

Figure 6. Top 10 significant GO gene sets from enrichment analysis using genes associated with any critical CpG sites in the promoter region (significant genes). Count: number of significant genes in a gene set. GeneRatio: the ratio between the number of significant genes in a gene set and the number of significant genes in GO.

marker and could not reflect the long-term exposure, which is critical for evaluating health effects accumulated through vaporing. DNA methylation is a well-established epigenetic biomarker, with unique profiles after exposure to air pollutants, heavy metals, and cigarette smoking [39, 40]. Our study represents the first investigation to explore the whole-genomic DNA methylation alterations in white blood cells after long-term e-cigarette exposure. Our results indicate that e-cigarettes induced extensive alteration of DNA methylation in white blood cells in a nicotine dose-dependent pattern. Several CpG methylated sites unique to e-cigarettes may be used as biomarkers to assess long-term e-cigarette exposure. For the first time, our results reveal the alteration of genome-wide DNA methylation of circulating white blood cells after long-term e-cigarette exposure. These findings provide strong evidence to support the use of DNA methylation as a potential biomarker for the health effects of e-cigarette exposure.

One unique design of our study is the dose-escalation, which is not easily evaluated by human e-cigarette vapers. However, dose escalation results are not only compelling

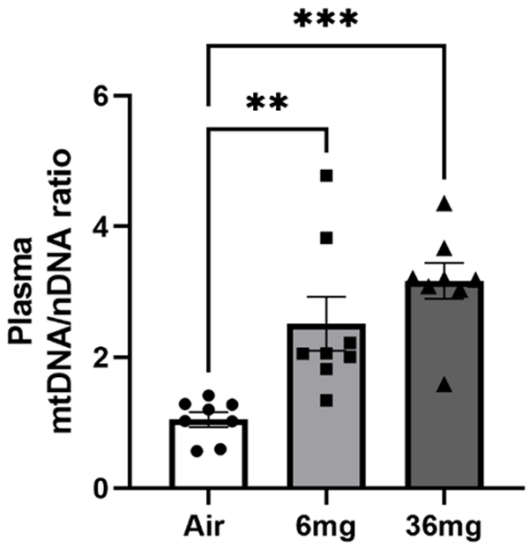

Figure 7. Increased mtDNA levels in the circulation after e-cigarette exposure. The ratio of mtDNA and nDNA indicates the mtDNA change after the E-cigarette exposure. For each group, N=8. Data points and error bars are means and SEMs, respectively, analyzed by Dunnett's multiple comparisons tests, **P<0.01; ***P<0.005, respectively.

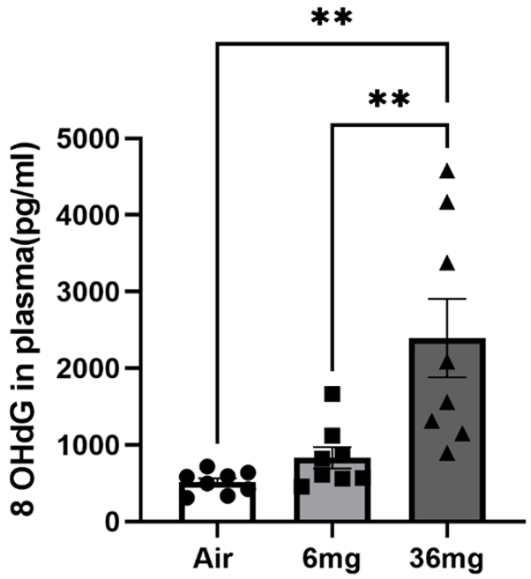

Figure 8. cell-free DNA oxidization after e-cigarette exposure. The value of the 8 OHdG indicates the level of DNA oxidization. For each group, N=8. Data points and error bars are means and SEMs, respectively, analyzed by Dunnett's multiple comparisons test, **P<0.01.

to confirm regulating effect of e-cigarettes on a CpG point but also have the potential to identify e-cigarette doses with less harmful health effects. Currently, no study in the current literature investigated dose-related DNA methylation effects of E-cigarette vaporing, and only a few studies discuss the dose-related methylation alterations in human smokers. In a study published in 2016, Zhang Y et al. demonstrated that methylation of 40 CpGs, mapped to 22 genes, was significantly associated with individual serum cotinine levels. The strongest association was found for *AHHR* cg05575921. A 10 ng/ml upregulation of cotinine resulted in a 3% lower methylation at *AHHR* cg05575921 [41]. This observation was confirmed by Prince C et al. in a study, which showed that methylations of cg05575921 and cg26703534 in smokers were both mapped to AHRR and strongly associated with blood cotinine levels [42]; dose-response in methylation at Cg05575921 was also related to the duration of smoking. In another study published in 2018, Park SL et al. showed increasing methylation beta-values of smokers in six CpG sites at higher levels of urinary nicotine metabolites. Four CpG sites were annotated in or near the FOXK2, PBX1, FNDC7, and FUBP3 genes; two other locations in non-annotated genetic regions [43].

The altered CpG site methylation status shown in our results overlapped with previous reports of DNA methylation after e-cigarette exposure. In a study including 117 smokers, 117 non-smokers, and 116 non-smoking vapers, epigenome-wide DNA methylation profiling from saliva revealed 7 CpG sites related to e-cigarette use at P<1×10-5. The CpG sites linked to e-cigarette use were largely distinct from those related to smoking. Consistent with this finding, our study showed that 3 out of those 7 genes, including acyl-CoA dehydrogenase 10 (ACAD10), semaphorin 5B, and immunoglobin superfamily member 21, also contained CpG sites with significantly altered methylation status [44]. Semaphorin 5B gene upregulation was also identified in another study using ApoE-/- mice after intermittent electronic cigarette exposure [34]. The altered CpG site methylation related to semaphorin 5B was also recognized in human smokers [45]. Previous studies also confirmed that 4 of the top 6 significant genes related to nicotine dosage in the e-cigarette, *Capns1*, *Znf598*, *Ccdc33,* and *Phc2*, were associated with cigarette smoking [25-30]. The

biological activities of these CpG site-associated genes are interesting. ACAD10 has been linked to type 2 diabetes [46] and hypertension [47]: ACAD10-deficient mice exhibited abnormal glucose tolerance and elevated insulin level, accumulated excess abdominal adipose tissue, and developed an early inflammatory liver process [48]. Phc2 was identified as a critical modulator of hematopoietic stem and progenitor cell (HSPC) trafficking. Genetic knockout of Phc2 in mice results in a severe defect in HSPC mobilization by depressing Vcam1 expression in bone marrow stromal cells, finally ending up with a systemic immunodeficiency [49].

Smoking is well known to be associated with systemic and local inflammation in the lungs, and higher tobacco consumption is associated with higher systemic inflammation both genetically and observationally [50]. Pro-inflammatory pathways are upregulated, and anti-inflammatory ones are downregulated for smoking exposure. Inflammatory cytokines such as TNFα, IL6, and RANTES are induced by smoking [51, 52]. The previous studies reported by our group and the others have shown that e-cigarette use/exposure results in systematic and local inflammation [32, 53]. The above observation correlates very well with the gene set enrichment KEGG pathway analysis, which showed MAPK signaling pathway is the most significant one in our study. It is conceivable that E-cigarette exposure induces a systematic pro-inflammatory environment by releasing growth factors and cytokines. These inflammatory agents activate the MAPK signaling pathways, further exacerbating the inflammatory process.

Mitochondria are organelles involved in many physiological and pathological functions. Recent evidence showed that it could also play a role as a regulator of the innate immune response [54]. mtDNA is ideal for inducing an innate immune response via its escape from the mitochondria to other organelles, the cytosol, and the extracellular space. Additionally, our previous study has shown cytoplasmic mtDNA activates toll-like receptor 9 in monocytes/macrophages and triggers the inflammatory process [32]. The released mtDNA in the cytosol could also be recognized by other DNA sensors, including cGAS, a cGAMP, whose activation leads to an enhanced expression of type I interferons and active pro-inflammatory cytokines IL-1β. Interaction of mtDNA with the cGAS-STING signaling axis has been described in multiple pathological conditions, which share the final common pathway of leakage of mtDNA from mitochondria to the cytosol [55]. Our data showed that cfDNA in the plasma contained more mtDNA after the E-cigarette exposure, illustrated by an increased mtDNA/ncDNA ratio, indicating that the damaged mtDNA was released from the cytoplasm to the plasma. In the DNA methylation profiling data, two mitochondrial function-related pathways have been affected based on the GO pathway analysis in the promotor region, including mitochondrial gene expression and mitochondrial translation. The dysfunction of mitochondria under the multiple stresses may cause the release of mtDNA, but the mechanisms triggering the release are still not fully understood. It is known that loss of mitophage [56] (selective autophagy process in which damaged mitochondria are targeted for lysosomal degradation), cytosolic ROS induced mitochondrial permeability transition [57], and opening of mitochondrial permeability transition pore [58] are several mechanisms for mtDNA release into the cytosol. Whether mitochondrial transcription and translocation are biomarkers for any of the mechanisms above is unknown. Elucidating the relationship between these pathways and the increased circulating mitochondrial DNA observed here will provide further insight into the cell-damaging effects of prolonged inhalation of e-cigarette aerosols.

In conclusion, our study reveals that e-cigarette exposure results in extensive DNA methylation alteration in male ApoE-/- mice in a dose-dependent manner of nicotine. Our epigenomic-wide CpG site methylation pattern overlaps with previously published methylation sites in vapers/smokers. The methylation pattern correlates well with enhanced systematic inflammation reported in animal models and human vapers.

Acknowledgements

This research was supported in part by a Career Enhancement Program Grant from the Yale Head and Neck SPORE, P50 DE030707.

Disclosure of conflict of interest

None.

Address correspondence to: Dr. He Wang, Yale University School of Medicine, 310 Cedar Street, New Haven, CT 06519, USA. E-mail: he.wang@yale.edu

References

[1] Krishnan-Sarin S, Jackson A, Morean M, Kong G, Bold KW, Camenga DR, Cavallo DA, Simon P and Wu R. E-cigarette devices used by high-school youth. Drug Alcohol Depend 2019; 194: 395-400.

[2] Fadus MC, Smith TT and Squeglia LM. The rise of e-cigarettes, pod mod devices, and JUUL among youth: factors influencing use, health implications, and downstream effects. Drug Alcohol Depend 2019; 201: 85-93.

[3] Parry A, Rulands S and Reik W. Active turnover of DNA methylation during cell fate decisions. Nat Rev Genet 2021; 22: 59-66.

[4] Caliri AW, Caceres A, Tommasi S and Besaratinia A. Hypomethylation of LINE-1 repeat elements and global loss of DNA hydroxymethylation in vapers and smokers. Epigenetics 2020; 15: 816-829.

[5] Suhre K and Zaghlool S. Connecting the epigenome, metabolome and proteome for a deeper understanding of disease. J Intern Med 2021; 290: 527-548.

[6] Bollepalli S, Korhonen T, Kaprio J, Anders S and Ollikainen M. EpiSmokEr: a robust classifier to determine smoking status from DNA methylation data. Epigenomics 2019; 11: 1469-1486.

[7] Joehanes R, Just AC, Marioni RE, Pilling LC, Reynolds LM, Mandaviya PR, Guan W, Xu T, Elks CE, Aslibekyan S, Moreno-Macias H, Smith JA, Brody JA, Dhingra R, Yousefi P, Pankow JS, Kunze S, Shah SH, McRae AF, Lohman K, Sha J, Absher DM, Ferrucci L, Zhao W, Demerath EW, Bressler J, Grove ML, Huan T, Liu C, Mendelson MM, Yao C, Kiel DP, Peters A, Wang-Sattler R, Visscher PM, Wray NR, Starr JM, Ding J, Rodriguez CJ, Wareham NJ, Irvin MR, Zhi D, Barrdahl M, Vineis P, Ambatipudi S, Uitterlinden AG, Hofman A, Schwartz J, Colicino E, Hou L, Vokonas PS, Hernandez DG, Singleton AB, Bandinelli S, Turner ST, Ware EB, Smith AK, Klengel T, Binder EB, Psaty BM, Taylor KD, Gharib SA, Swenson BR, Liang L, DeMeo DL, O'Connor GT, Herceg Z, Ressler KJ, Conneely KN, Sotoodehnia N, Kardia SL, Melzer D, Baccarelli AA, van Meurs JB, Romieu I, Arnett DK, Ong KK, Liu Y, Waldenberger M, Deary IJ, Fornage M, Levy D and London SJ. Epigenetic signatures of cigarette smoking. Circ Cardiovasc Genet 2016; 9: 436-447.

[8] McCartney DL, Stevenson AJ, Hillary RF, Walker RM, Bermingham ML, Morris SW, Clarke TK, Campbell A, Murray AD, Whalley HC, Porteous DJ, Visscher PM, McIntosh AM, Evans KL, Deary IJ and Marioni RE. Epigenetic signatures of starting and stopping smoking. EBioMedicine 2018; 37: 214-220.

[9] Zeilinger S, Kuhnel B, Klopp N, Baurecht H, Kleinschmidt A, Gieger C, Weidinger S, Lattka E, Adamski J, Peters A, Strauch K, Waldenberger M and Illig T. Tobacco smoking leads to extensive genome-wide changes in DNA methylation. PLoS One 2013; 8: e63812.

[10] Ligthart S, Marzi C, Aslibekyan S, Mendelson MM, Conneely KN, Tanaka T, Colicino E, Waite LL, Joehanes R, Guan W, Brody JA, Elks C, Marioni R, Jhun MA, Agha G, Bressler J, Ward-Caviness CK, Chen BH, Huan T, Bakulski K and Salfati EL; WHI-EMPC Investigators, Fiorito G; CHARGE epigenetics of Coronary Heart Disease, Wahl S, Schramm K, Sha J, Hernandez DG, Just AC, Smith JA, Sotoodehnia N, Pilling LC, Pankow JS, Tsao PS, Liu C, Zhao W, Guarrera S, Michopoulos VJ, Smith AK, Peters MJ, Melzer D, Vokonas P, Fornage M, Prokisch H, Bis JC, Chu AY, Herder C, Grallert H, Yao C, Shah S, McRae AF, Lin H, Horvath S, Fallin D, Hofman A, Wareham NJ, Wiggins KL, Feinberg AP, Starr JM, Visscher PM, Murabito JM, Kardia SL, Absher DM, Binder EB, Singleton AB, Bandinelli S, Peters A, Waldenberger M, Matullo G, Schwartz JD, Demerath EW, Uitterlinden AG, van Meurs JB, Franco OH, Chen YI, Levy D, Turner ST, Deary IJ, Ressler KJ, Dupuis J, Ferrucci L, Ong KK, Assimes TL, Boerwinkle E, Koenig W, Arnett DK, Baccarelli AA, Benjamin EJ and Dehghan A. DNA methylation signatures of chronic low-grade inflammation are associated with complex diseases. Genome Biol 2016; 17: 255.

[11] Andersen A, Reimer R, Dawes K, Becker A, Hutchens N, Miller S, Dogan M, Hundley B, J AM, J DL and Philibert R. DNA methylation differentiates smoking from vaping and non-combustible tobacco use. Epigenetics 2022; 17: 178-190.

[12] Song MA, Freudenheim JL, Brasky TM, Mathe EA, McElroy JP, Nickerson QA, Reisinger SA, Smiraglia DJ, Weng DY, Ying KL, Wewers MD and Shields PG. Biomarkers of exposure and effect in the lungs of smokers, non-smokers, and electronic cigarette users. Cancer Epidemiol Biomarkers Prev 2020; 29: 443-451.

[13] Liang L, Willis-Owen SAG, Laprise C, Wong KCC, Davies GA, Hudson TJ, Binia A, Hopkin JM, Yang IV, Grundberg E, Busche S, Hudson M, Ronnblom L, Pastinen TM, Schwartz DA, Lathrop GM, Moffatt MF and Cookson WOCM. An epigenome-wide association study of total serum immunoglobulin E concentration. Nature 2015; 520: 670-674.

[14] Juvinao-Quintero DL, Marioni RE, Ochoa-Rosales C, Russ TC, Deary IJ, van Meurs JBJ, Voortman T, Hivert MF, Sharp GC, Relton CL and Elliott HR. DNA methylation of blood cells is associated with prevalent type 2 diabetes in a meta-analysis of four European cohorts. Clin Epigenetics 2021; 13: 40.

[15] Orozco LD, Farrell C, Hale C, Rubbi L, Rinaldi A, Civelek M, Pan C, Lam L, Montoya D, Edillor C, Seldin M, Boehnke M, Mohlke KL, Jacobsen S, Kuusisto J, Laakso M, Lusis AJ and Pellegrini M. Epigenome-wide association in adipose tissue from the METSIM cohort. Hum Mol Genet 2018; 27: 2586.

[16] Locke AE, Kahali B, Berndt SI, Justice AE, Pers TH, Day FR, Powell C, Vedantam S, Buchkovich ML, Yang J, Croteau-Chonka DC, Esko T, Fall T, Ferreira T, Gustafsson S, Kutalik Z, Luan J, Magi R, Randall JC, Winkler TW, Wood AR, Workalemahu T, Faul JD, Smith JA, Zhao JH, Zhao W, Chen J, Fehrmann R, Hedman AK, Karjalainen J, Schmidt EM, Absher D, Amin N, Anderson D, Beekman M, Bolton JL, Bragg-Gresham JL, Buyske S, Demirkan A, Deng G, Ehret GB, Feenstra B, Feitosa MF, Fischer K, Goel A, Gong J, Jackson AU, Kanoni S, Kleber ME, Kristiansson K, Lim U, Lotay V, Mangino M, Leach IM, Medina-Gomez C, Medland SE, Nalls MA, Palmer CD, Pasko D, Pechlivanis S, Peters MJ, Prokopenko I, Shungin D, Stancakova A, Strawbridge RJ, Sung YJ, Tanaka T, Teumer A, Trompet S, van der Laan SW, van Setten J, Van Vliet-Ostaptchouk JV, Wang Z, Yengo L, Zhang W, Isaacs A, Albrecht E, Arnlov J, Arscott GM, Attwood AP, Bandinelli S, Barrett A, Bas IN, Bellis C, Bennett AJ, Berne C, Blagieva R, Bluher M, Bohringer S, Bonnycastle LL, Bottcher Y, Boyd HA, Bruinenberg M, Caspersen IH, Chen YI, Clarke R, Daw EW, de Craen AJM, Delgado G, Dimitriou M, Doney ASF, Eklund N, Estrada K, Eury E, Folkersen L, Fraser RM, Garcia ME, Geller F, Giedraitis V, Gigante B, Go AS, Golay A, Goodall AH, Gordon SD, Gorski M, Grabe HJ, Grallert H, Grammer TB, Grassler J, Gronberg H, Groves CJ, Gusto G, Haessler J, Hall P, Haller T, Hallmans G, Hartman CA, Hassinen M, Hayward C, Heard-Costa NL, Helmer Q, Hengstenberg C, Holmen O, Hottenga JJ, James AL, Jeff JM, Johansson A, Jolley J, Juliusdottir T, Kinnunen L, Koenig W, Koskenvuo M, Kratzer W, Laitinen J, Lamina C, Leander K, Lee NR, Lichtner P, Lind L, Lindstrom J, Lo KS, Lobbens S, Lorbeer R, Lu Y, Mach F, Magnusson PKE, Mahajan A, McArdle WL, McLachlan S, Menni C, Merger S, Mihailov E, Milani L, Moayyeri A, Monda KL, Morken MA, Mulas A, Muller G, Muller-Nurasyid M, Musk AW, Nagaraja R, Nothen MM, Nolte IM, Pilz S, Rayner NW, Renstrom F, Rettig R, Ried JS, Ripke S, Robertson NR, Rose LM, Sanna S, Scharnagl H, Scholtens S, Schumacher FR, Scott WR, Seufferlein T, Shi J, Smith AV, Smolonska J, Stanton AV, Steinthorsdottir V, Stirrups K, Stringham HM, Sundstrom J, Swertz MA, Swift AJ, Syvanen AC, Tan ST, Tayo BO, Thorand B, Thorleifsson G, Tyrer JP, Uh HW, Vandenput L, Verhulst FC, Vermeulen SH, Verweij N, Vonk JM, Waite LL, Warren HR, Waterworth D, Weedon MN, Wilkens LR, Willenborg C, Wilsgaard T, Wojczynski MK, Wong A, Wright AF, Zhang Q, LifeLines Cohort S, Brennan EP, Choi M, Dastani Z, Drong AW, Eriksson P, Franco-Cereceda A, Gadin JR, Gharavi AG, Goddard ME, Handsaker RE, Huang J, Karpe F, Kathiresan S, Keildson S, Kiryluk K, Kubo M, Lee JY, Liang L, Lifton RP, Ma B, McCarroll SA, McKnight AJ, Min JL, Moffatt MF, Montgomery GW, Murabito JM, Nicholson G, Nyholt DR, Okada Y, Perry JRB, Dorajoo R, Reinmaa E, Salem RM, Sandholm N, Scott RA, Stolk L, Takahashi A, Tanaka T, van 't Hooft FM, Vinkhuyzen AAE, Westra HJ, Zheng W, Zondervan KT; ADIPOGen Consortium; AGEN-BMI Working Group; CARDIOGRAMplusC4D Consortium; CKDGen Consortium; GLGC; ICBP; MAGIC Investigators; MuTHER Consortium; MIGen Consortium; PAGE Consortium; ReproGen Consortium; GENIE Consortium; International Endogene Consortium, Heath AC, Arveiler D, Bakker SJL, Beilby J, Bergman RN, Blangero J, Bovet P, Campbell H, Caulfield MJ, Cesana G, Chakravarti A, Chasman DI, Chines PS, Collins FS, Crawford DC, Cupples LA, Cusi D, Danesh J, de Faire U, den Ruijter HM, Dominiczak AF, Erbel R, Erdmann J, Eriksson JG, Farrall M, Felix SB, Ferrannini E, Ferrieres J, Ford I, Forouhi NG, Forrester T, Franco OH, Gansevoort RT, Gejman PV, Gieger C, Gottesman O, Gudnason V, Gyllensten U, Hall AS, Harris TB, Hattersley AT, Hicks AA, Hindorff LA, Hingorani AD, Hofman A, Homuth G, Hovingh GK, Humphries SE, Hunt SC, Hypponen E, Illig T, Jacobs KB, Jarvelin MR, Jockel KH, Johansen B, Jousilahti P, Jukema JW, Jula AM, Kaprio J, Kastelein JJP, Keinanen-Kiukaanniemi SM, Kiemeney LA, Knekt P, Kooner JS, Kooperberg C, Kovacs P, Kraja AT, Kumari M, Kuusisto J, Lakka TA, Langenberg C, Marchand LL, Lehtimaki T, Lyssenko V, Mannisto S, Marette A, Matise TC, McKenzie CA, McKnight B, Moll FL, Morris AD, Morris AP, Murray JC, Nelis M, Ohlsson C, Oldehinkel AJ, Ong KK, Madden PAF, Pasterkamp G, Peden JF, Peters A, Postma DS, Pramstaller PP, Price JF, Qi L, Raitakari OT, Rankinen T, Rao DC, Rice TK, Ridker PM, Rioux JD, Ritchie MD, Rudan I, Salomaa V, Samani NJ, Saramies J, Sarzynski MA, Schunkert H,

Schwarz PEH, Sever P, Shuldiner AR, Sinisalo J, Stolk RP, Strauch K, Tonjes A, Tregouet DA, Tremblay A, Tremoli E, Virtamo J, Vohl MC, Volker U, Waeber G, Willemsen G, Witteman JC, Zillikens MC, Adair LS, Amouyel P, Asselbergs FW, Assimes TL, Bochud M, Boehm BO, Boerwinkle E, Bornstein SR, Bottinger EP, Bouchard C, Cauchi S, Chambers JC, Chanock SJ, Cooper RS, de Bakker PIW, Dedoussis G, Ferrucci L, Franks PW, Froguel P, Groop LC, Haiman CA, Hamsten A, Hui J, Hunter DJ, Hveem K, Kaplan RC, Kivimaki M, Kuh D, Laakso M, Liu Y, Martin NG, Marz W, Melbye M, Metspalu A, Moebus S, Munroe PB, Njolstad I, Oostra BA, Palmer CNA, Pedersen NL, Perola M, Perusse L, Peters U, Power C, Quertermous T, Rauramaa R, Rivadeneira F, Saaristo TE, Saleheen D, Sattar N, Schadt EE, Schlessinger D, Slagboom PE, Snieder H, Spector TD, Thorsteinsdottir U, Stumvoll M, Tuomilehto J, Uitterlinden AG, Uusitupa M, van der Harst P, Walker M, Wallaschofski H, Wareham NJ, Watkins H, Weir DR, Wichmann HE, Wilson JF, Zanen P, Borecki IB, Deloukas P, Fox CS, Heid IM, O'Connell JR, Strachan DP, Stefansson K, van Duijn CM, Abecasis GR, Franke L, Frayling TM, McCarthy MI, Visscher PM, Scherag A, Willer CJ, Boehnke M, Mohlke KL, Lindgren CM, Beckmann JS, Barroso I, North KE, Ingelsson E, Hirschhorn JN, Loos RJF and Speliotes EK. Genetic studies of body mass index yield new insights for obesity biology. Nature 2015; 518: 197-206.

[17] Xu ZL, Niu L, Li LP and Taylor JA. ENmix: a novel background correction method for Illumina HumanMethylation450 BeadChip. Nucleic Acids Res 2016; 44: e20.

[18] Xu ZL, Langie SA, De Boever P, Taylor JA and Niu L. RELIC: a novel dye-bias correction method for Illumina Methylation BeadChip. BMC Genomics 2017; 18: 4.

[19] Du P, Zhang X, Huang CC, Jafari N, Kibbe WA, Hou LF and Lin SM. Comparison of Beta-value and M-value methods for quantifying methylation levels by microarray analysis. BMC Bioinformatics 2010; 11: 587.

[20] Wu TZ, Hu EQ, Xu SB, Chen MJ, Guo PF, Dai ZH, Feng TZ, Zhou L, Tang WL, Zhan L, Fu XC, Liu SS, Bo XC and Yu GC. clusterProfiler 4.0: a universal enrichment tool for interpreting omics data. Innovation (Camb) 2021; 2: 100141.

[21] Richmond BW, Brucker RM, Han W, Du RH, Zhang Y, Cheng DS, Gleaves L, Abdolrasulnia R, Polosukhina D, Clark PE, Bordenstein SR, Blackwell TS and Polosukhin VV. Airway bacteria drive a progressive COPD-like phenotype in mice with polymeric immunoglobulin receptor deficiency. Nat Commun 2016; 7: 11240.

[22] Noel A, Verret CM, Hasan F, Lomnicki S, Morse J, Robichaud A and Penn AL. Generation of electronic cigarette aerosol by a third-generation machine-vaping device: application to toxicological studies. J Vis Exp 2018; 58095.

[23] Pidsley R, Zotenko E, Peters TJ, Lawrence MG, Risbridger GP, Molloy P, Van Djik S, Muhlhausler B, Stirzaker C and Clark SJ. Critical evaluation of the Illumina MethylationEPIC BeadChip microarray for whole-genome DNA methylation profiling. Genome Biol 2016; 17: 208.

[24] Garcia-Prieto CA, Alvarez-Errico D, Musulen E, Bueno-Costa A, N Vazquez B, Vaquero A and Esteller M. Validation of a DNA methylation microarray for 285,000 CpG sites in the mouse genome. Epigenetics 2022; 1-9.

[25] Duclos GE, Teixeira VH, Autissier P, Gesthalter YB, Reinders-Luinge MA, Terrano R, Dumas YM, Liu G, Mazzilli SA, Brandsma CA, van den Berge M, Janes SM, Timens W, Lenburg ME, Spira A, Campbell JD and Beane J. Characterizing smoking-induced transcriptional heterogeneity in the human bronchial epithelium at single-cell resolution. Sci Adv 2019; 5: eaaw3413.

[26] Ryan DM, Vincent TL, Salit J, Walters MS, Agosto-Perez F, Shaykhiev R, Strulovici-Barel Y, Downey RJ, Buro-Auriemma LJ, Staudt MR, Hackett NR, Mezey JG and Crystal RG. Smoking dysregulates the human airway basal cell transcriptome at COPD risk locus 19q13.2. PLoS One 2014; 9: e88051.

[27] Beane J, Sebastiani P, Liu G, Brody JS, Lenburg ME and Spira A. Reversible and permanent effects of tobacco smoke exposure on airway epithelial gene expression. Genome Biol 2007; 8: R201.

[28] Fowler PA, Childs AJ, Courant F, MacKenzie A, Rhind SM, Antignac JP, Le Bizec B, Filis P, Evans F, Flannigan S, Maheshwari A, Bhattacharya S, Monteiro A, Anderson RA and O'Shaughnessy PJ. In utero exposure to cigarette smoke dysregulates human fetal ovarian developmental signalling. Hum Reprod 2014; 29: 1471-1489.

[29] Song WC, Lin GN, Yu SY and Zhao M. Genome-wide identification of the shared genetic basis of cannabis and cigarette smoking and schizophrenia implicates NCAM1 and neuronal abnormality. Psychiatry Res 2022; 310: 114453.

[30] Marczylo EL, Amoako AA, Konje JC, Gant TW and Marczylo TH. Smoking induces differential miRNA expression in human spermatozoa: a potential transgenerational epigenetic concern? Epigenetics 2012; 7: 432-439.

[31] Mancuso N, Shi H, Goddard P, Kichaev G, Gusev A and Pasaniuc B. Integrating gene expression with summary association statistics

to identify genes associated with 30 complex traits. Am J Hum Genet 2017; 100: 473-487.
[32] Li JL, Huynh L, Cornwell WD, Tang MS, Simborio H, Huang J, Kosmider B, Rogers TJ, Zhao HQ, Steinberg MB, Thu Thi Le L, Zhang LJ, Pham K, Liu C and Wang H. Electronic cigarettes induce mitochondrial DNA damage and trigger TLR9 (Toll-Like Receptor 9)-mediated atherosclerosis. Arterioscler Thromb Vasc Biol 2021; 41: 839-853.
[33] Getiye Y, Peterson MR, Phillips BD, Carrillo D, Bisha B and He GL. E-cigarette exposure with or without heating the e-liquid induces differential remodeling in the lungs and right heart of mice. J Mol Cell Cardiol 2022; 168: 83-95.
[34] Espinoza-Derout J, Hasan KM, Shao XM, Jordan MC, Sims C, Lee DL, Sinha S, Simmons Z, Mtume N, Liu Y, Roos KP, Sinha-Hikim AP and Friedman TC. Chronic intermittent electronic cigarette exposure induces cardiac dysfunction and atherosclerosis in apolipoprotein-E knockout mice. Am J Physiol Heart Circ Physiol 2019; 317: H445-H459.
[35] Tumburu L, Ghosh-Choudhary S, Seifuddin FT, Barbu EA, Yang S, Ahmad MM, Wilkins LHW, Tunc I, Sivakumar I, Nichols JS, Dagur PK, Yang S, Almeida LEF, Quezado ZMN, Combs CA, Lindberg E, Bleck CKE, Zhu J, Shet AS, Chung JH, Pirooznia M and Thein SL. Circulating mitochondrial DNA is a pro-inflammatory DAMP in sickle cell disease. Blood 2021; 137: 3116-3126.
[36] Wiersma M, van Marion DMS, Bouman EJ, Li J, Zhang D, Ramos KS, Lanters EAH, de Groot NMS and Brundel BJJM. Cell-free circulating mitochondrial DNA: a potential blood-based marker for atrial fibrillation. Cells 2020; 9: 1159.
[37] Liu J, Cai XM, Xie L, Tang Y, Cheng JH, Wang J, Wang LJ and Gong JB. Circulating cell free mitochondrial DNA is a biomarker in the development of coronary heart disease in the patients with Type 2 diabetes. Clin Lab 2015; 61: 661-667.
[38] Muthumalage T, Lamb T, Friedman MR and Rahman I. E-cigarette flavored pods induce inflammation, epithelial barrier dysfunction, and DNA damage in lung epithelial cells and monocytes. Sci Rep 2019; 9: 19035.
[39] Martin EM and Fry RC. Environmental influences on the epigenome: exposure- associated DNA methylation in human populations. Annu Rev Public Health 2018; 39: 309-333.
[40] Long PP, Wang QH, Zhang YZ, Zhu XY, Yu K, Jiang HJ, Liu XZ, Zhou M, Yuan Y, Liu K, Jiang J, Zhang XM, He MA, Guo H, Chen WH, Yuan J, Cheng LX, Liang LM and Wu TC. Profile of copper-associated DNA methylation and its association with incident acute coronary syndrome. Clin Epigenetics 2021; 13: 19.
[41] Zhang Y, Florath I, Saum KU and Brenner H. Self-reported smoking, serum cotinine, and blood DNA methylation. Environ Res 2016; 146: 395-403.
[42] Prince C, Hammerton G, Taylor AE, Anderson EL, Timpson NJ, Davey Smith G, Munafo MR, Relton CL and Richmond RC. Investigating the impact of cigarette smoking behaviours on DNA methylation patterns in adolescence. Hum Mol Genet 2019; 28: 155-165.
[43] Park SL, Patel YM, Loo LWM, Mullen DJ, Offringa IA, Maunakea A, Stram DO, Siegmund K, Murphy SE, Tiirikainen M and Le Marchand L. Association of internal smoking dose with blood DNA methylation in three racial/ethnic populations. Clin Epigenetics 2018; 10: 110.
[44] Richmond RC, Sillero-Rejon C, Khouja JN, Prince C, Board A, Sharp G, Suderman M, Relton CL, Munafo M and Gage SH. Investigating the DNA methylation profile of e-cigarette use. Clin Epigenetics 2021; 13: 183.
[45] Gupta R, van Dongen J, Fu Y, Abdellaoui A, Tyndale RF, Velagapudi V, Boomsma DI, Korhonen T, Kaprio J, Loukola A and Ollikainen M. Epigenome-wide association study of serum cotinine in current smokers reveals novel genetically driven loci. Clin Epigenetics 2019; 11: 1.
[46] Bian L, Hanson RL, Muller YL and Ma L; MAGIC Investigators, Kobes S, Knowler WC, Bogardus C and Baier LJ. Variants in ACAD10 are associated with type 2 diabetes, insulin resistance and lipid oxidation in Pima Indians. Diabetologia 2010; 53: 1349-1353.
[47] Yamada Y, Sakuma J, Takeuchi I, Yasukochi Y, Kato K, Oguri M, Fujimaki T, Horibe H, Muramatsu M, Sawabe M, Fujiwara Y, Taniguchi Y, Obuchi S, Kawai H, Shinkai S, Mori S, Arai T and Tanaka M. Identification of polymorphisms in 12q24.1, ACAD10, and BRAP as novel genetic determinants of blood pressure in Japanese by exome-wide association studies. Oncotarget 2017; 8: 43068-43079.
[48] Bloom K, Mohsen AW, Karunanidhi A, El Demellawy D, Reyes-Mugica M, Wang Y, Ghaloul-Gonzalez L, Otsubo C, Tobita K, Muzumdar R, Gong Z, Tas E, Basu S, Chen J, Bennett M, Hoppel C and Vockley J. Investigating the link of ACAD10 deficiency to type 2 diabetes mellitus. J Inherit Metab Dis 2018; 41: 49-57.
[49] Bae J, Choi SP, Isono K, Lee JY, Park SW, Choi CY, Han J, Kim SH, Lee HH, Park K, Jin HY, Lee SJ, Park CG, Koseki H, Lee YS and Chun T. Phc2 controls hematopoietic stem and progenitor cell mobilization from bone marrow by repressing Vcam1 expression. Nat Commun 2019; 10: 3496.
[50] Colak Y, Afzal S, Lange P and Nordestgaard BG. Smoking, systemic inflammation, and airflow limitation: a mendelian randomization

analysis of 98 085 individuals from the general population. Nicotine Tob Res 2019; 21: 1036-1044.
[51] Gomes M, Teixeira AL, Coelho A, Araujo A and Medeiros R. The role of inflammation in lung cancer. Adv Exp Med Biol 2014; 816: 1-23.
[52] Coussens LM and Werb Z. Inflammation and cancer. Nature 2002; 420: 860-867.
[53] Kotoulas SC, Pataka A, Domvri K, Spyratos D, Katsaounou P, Porpodis K, Fouka E, Markopoulou A, Passa-Fekete K, Grigoriou I, Kontakiotis T, Argyropoulou P and Papakosta D. Acute effects of e-cigarette vaping on pulmonary function and airway inflammation in healthy individuals and in patients with asthma. Respirology 2020; 25: 1037-1045.
[54] Herst PM, Rowe MR, Carson GM and Berridge MV. Functional mitochondria in health and disease. Front Endocrinol (Lausanne) 2017; 8: 296.
[55] De Gaetano A, Solodka K, Zanini G, Selleri V, Mattioli AV, Nasi M and Pinti M. Molecular mechanisms of mtDNA-mediated inflammation. Cells 2021; 10: 2898.
[56] Harris J, Deen N, Zamani S and Hasnat MA. Mitophagy and the release of inflammatory cytokines. Mitochondrion 2018; 41: 2-8.
[57] Bernardi P. The mitochondrial permeability transition pore: a mystery solved? Front Physiol 2013; 4: 95.
[58] Yu CH, Davidson S, Harapas CR, Hilton JB, Mlodzianoski MJ, Laohamonthonkul P, Louis C, Low RRJ, Moecking J, De Nardo D, Balka KR, Calleja DJ, Moghaddas F, Ni E, McLean CA, Samson AL, Tyebji S, Tonkin CJ, Bye CR, Turner BJ, Pepin G, Gantier MP, Rogers KL, McArthur K, Crouch PJ and Masters SL. TDP-43 triggers mitochondrial DNA release via mPTP to activate cGAS/STING in ALS. Cell 2020; 183: 636-649, e18.

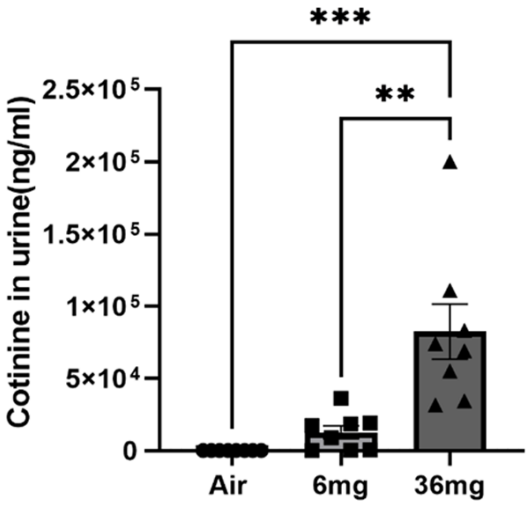

Figure S1. Measurement of urine cotinine level after 14 weeks E-cigarette exposure. Cotinine level change column after E-cigarette exposure. For each group, N=8. Data points and error bars are means and SEMs, respectively, analyzed by Dunnett's multiple comparisons tests; **P<0.01; ***P<0.005, respectively.

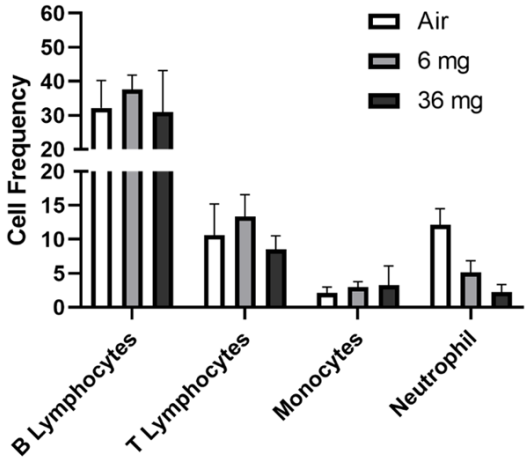

Figure S2. Flow cytometry analysis of white blood cell composition after 14 weeks of E-cigarette exposure. Column of the cell frequency for each cell type, N=3 for each group, no significant cell type change after E-cigarette exposure.

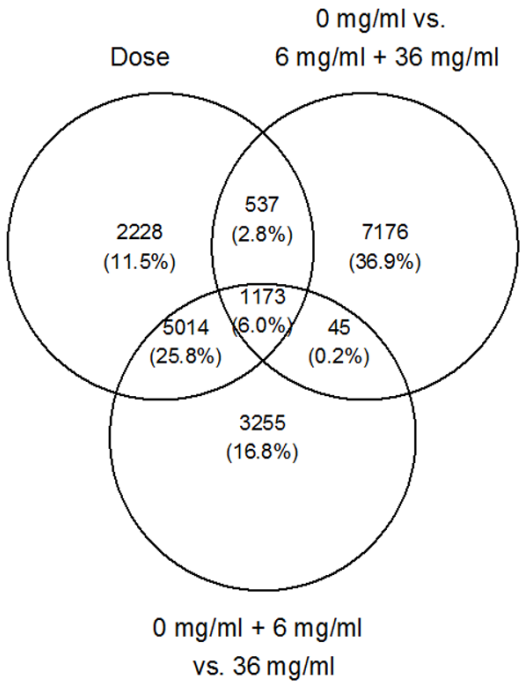

Figure S3. Venn graph to show the overlaps of significant CpG sites from dose analysis, comparing 0 mg/ml group to 6 mg/ml + 36 mg/ml groups, and comparing 0 mg/ml + 6 mg/ml groups to 36 mg/ml group.

Table S4. Significant KEGG pathways when using genes that are associated with any significant CpG sites for the enrichment analysis

ID	Description	GeneRatio	BgRatio	*P* value	FDR	geneID	Count
mmu04261	Adrenergic signaling in cardiomyocytes	79/2380	239/11633	2.87E-06	0.00049138	Q5SW28/P97718/Q8BUE5/Q9Z1L5/Q01815/Q0PCR6/P09542/P23299/Q545H6/P97490/Q923T9/Q8VHW3/Q9R0K7/Q3UHH0/Q8BH52/Q9Z125/A0A0R4J082/P10417/P20444/Q4VA93/Q9JJV4/Q9WUI1/P11798/Q9DBL0/Q9ERT9/P0DP27/P0DP28/Q8CC27/P97414/Q60996/S4R2P9/Q99246/Q6PHS9/Q6PHZ2/B2RXC8/P50752/Q6P3Z7/Q54AB6/P27699/Q8VCC8/P84309/A3K-GF7/P68181/Q02789/Q76MZ3/P08752/Q64518/Q8R0X5/Q91Z83/Q6Q477/P58774/Q9Z1B7/P51667/P61014/P63094/P58771/Q545Y3/Q5RJF7/F8VPL1/Q9EQZ6/P62715/Q01341/F8VQ52/Q9WUA6/O88602/Q3ZB20/Q7TNP2/O08532/Q14BH8/Q7M729/Q8K596/Q8R3Z5/A2A545/P48787/Q497F1/Q6PD03/B1AYL1/Q9JJV9/K3W4N7	79
mmu04010	MAPK signaling pathway	138/2380	474/11633	3.01E-06	0.00049138	P48455/Q3UFB7/Q9Z1L5/Q0VG15/Q01815/Q0PCR6/Q8CE90/O35608/Q1HKZ5/Q03145/P25118/Q3U479/P97820/A0A0A6YWR8/P20826/Q62312/Q61696/P16627/Q9JI11/P70424/Q8VHW3/E9Q7P2/P14404/P15209/Q9ESL4/Q9WTK5/P18653/Q8BYC6/P20444/Q4VA93/Q9JJV4/Q62132/Q9WUI1/Q9D7X3/Q925I7/P31938/Q3TMJ8/Q8BWG8/P01132/P52801/Q04690/P41158/Q8CC27/P27090/Q99246/P61148/Q6ZWS1/Q9WVS7/O55017/P21237/Q541P3/Q6PHS9/P09535/Q99K90/P32883/Q5J7N1/P28028/Q04863/A0A0A0MQ87/F8VQL0/P68181/P17156/Q8BTM9/P30306/Q3U535/Q9DBN8/Q02789/P31240/A0A0R4IZW4/Q62073/P60764/Q14A12/Q9WUL6/O09112/O08989/Q3TPX5/Q80X90/O35099/Q9Z1B7/Q91Y86/P22339/Q61526/P54830/O08605/A2A8W8/A0A087WS83/Q549C9/P27671/Q9ESN9/P36993/Q5RJF7/F8VPL1/P47809/Q543X6/Q9WUT3/Q9WVI9/Q02858/P97953/P15655/Q541T2/Q9WUA6/P26618/O88602/Q3ZB20/Q3UMW7/P49138/Q3U2P8/O08532/Q14BH8/Q64729/P01139/A0A0A0MQ82/Q9ESS0/Q91Z46/P63318/Q3UN66/P21803/E9QK53/P62071/P13504/Q32MH0/P10637/O35613/Q3UKR0/P10749/Q9QUG9/Q8R3Z5/A2A545/Q50L42/P63001/P17879/O08543/Q61161/Q8CFN5/Q7TSI8/P97445/P35639/Q9Z1S3	138
mmu04520	Adherens junction	46/2380	121/11633	6.15E-06	0.00067065	Q8BUN5/Q62417/Q924A0/E9QQ91/Q9QUI0/Q65CL1/Q9JLB9/Q62312/P70424/Q9JKF1/Q99NH2/A0A0R4J1Y4/Q64727/B2RU80/Q9Z1J1/A1A550/A2A8L5/P39688/Q7TPR4/Q02248/Q9JKF6/F8VQL0/Q64455/E9Q4S7/P28828/Q68FM4/Q62073/P60764/Q14A12/P30999/P39447/F8VPR5/Q8BH43/P70451/Q3TZJ5/E9QNA7/Q64729/Q04736/Q3TJI7/Q9D358/Q561M1/Q61301/P63001/P27782/Q3TYB0/Q8BGZ9	46
mmu05414	Dilated cardiomyopathy	54/2380	153/11633	1.31E-05	0.00107134	Q9Z1L5/Q01815/Q0PCR6/A2A864/P09542/P97490/Q8VHW3/Q9JJV4/Q62470/Q8CC27/Q3TZS3/S4R2P9/P27090/Q99246/Q6PHS9/P50752/Q6P3Z7/Q54AB6/P84309/P68181/Q02789/Q64518/Q8R0X5/Q91Z83/P58774/P51667/E9PXZ3/P61014/A0A0B4J1F0/P63094/Q62165/P58771/Q545Y3/Q5RJF7/F8VPL1/Q01341/F8VQ52/O88602/Q3ZB20/O08532/Q14BH8/P82347/P19137/B8JK39/P11688/Q0VBD0/O70309/Q6PE70/Q8K596/Q8R3Z5/A2A545/Q60675/P48787/Q497F1	54
mmu04360	Axon guidance	82/2380	261/11633	1.65E-05	0.00107822	Q80TR4/P22726/P48455/Q69ZX8/Q812A2/F8VPQ4/Q9JI33/Q8BL65/Q62178/Q03145/Q9WVB4/Q76I79/O08644/Q9QUI0/Q8K120/Q923T9/P70206/Q8K1S3/Q62181/Q99NH2/A0A0R4J1Y4/Q8R4F1/P20444/Q4VA93/P11798/Q9DC04/Q8CBF3/Q8CA63/P52801/P43029/P39688/Q8C031/Q99PH1/Q6PHZ2/Q6PCX7/O55222/P23359/Q60591/P97333/Q80UG2/P32883/Q5J7N1/Q76KF0/Q8K330/P45591/Q3UHW9/F8VQL0/Q62226/Q60519/Q5SW75/P52800/Q4FJM3/G1K381/P08752/P60764/Q14A12/O88632/Q60629/P00520/P54763/B2RXS4/O09118/P54754/O09126/Q03137/Q91Z69/Q9QUQ5/Q9JK84/Q8CIH5/D3Z4M6/Q9QUR8/Q8CHT1/E9QK62/O08747/Q8K4G5/E9QK41/M9MMK0/O54785/O35904/P63001/O08543/P35235	82
mmu05410	Hypertrophic cardiomyopathy	53/2380	152/11633	2.32E-05	0.00126214	Q9Z1L5/Q01815/Q0PCR6/A2A864/P09542/Q91WG5/O54950/Q3TWR3/Q8VHW3/Q9JJV4/Q6PAM0/Q62470/Q8CC27/Q3TZS3/S4R2P9/P27090/Q99246/Q6PHS9/P50752/Q6P3Z7/Q54AB6/Q02789/Q64518/Q8R0X5/Q91Z83/P58774/P51667/E9PXZ3/A0A0B4J1F0/Q62165/P58771/Q545Y3/Q5RJF7/F8VPL1/O88602/Q3ZB20/O08532/Q14BH8/P82347/P19137/B8JK39/P09470/Q3TU20/P11688/Q0VBD0/O70309/Q6PE70/Q8K596/Q8R3Z5/A2A545/Q60675/P48787/Q497F1	53

mmu04070	Phosphatidylinositol signaling system	44/2380	121/11633	3.52E-05	0.00164624	Q7TT16/E9QAN8/Q8CDA1/P20444/Q4VA93/Q8K3R3/Q9EPW0/F6V2U0/Q3UEQ1/P0DP27/P0DP28/Q6ZQB6/Q7TNC9/P98191/Q9R1C6/Q6P549/Q7TS72/E9Q7S0/Q8BYN3/Q6PD10/A3KGF7/O88673/D3YXJ0/Q8BKC8/D3YWQ0/E9PUQ8/P70227/Q8R3B1/B2RXC2/O70167/Q80XI4/Q8CIH5/O70161/Q9D2G5/Q9ES52/Q8CBQ5/Q6NS52/A2ARP1/P63318/Q3UN66/Q99L43/O35904/Q91WG7/P11881	44
mmu04020	Calcium signaling pathway	105/2380	360/11633	4.18E-05	0.00170898	P97718/Q8BUE5/P48455/Q3UFB7/O08786/Q0VG15/Q01815/Q0PCR6/Q01098/Q60613/Q9Z0J4/P97490/Q923T9/P35438/P70424/Q9R0K7/Q3UHH0/E9Q7P2/P15209/Q9QVP9/Q3UDE9/Q03391/Q62463/Q3UMR5/Q02152/P20444/Q4VA93/Q8BWG9/P11798/Q9DBL0/Q925I7/Q8K3R3/P30678/P01132/Q9ERZ4/P0DP27/P0DP28/S4R2P9/Q99246/P61148/Q6ZWS1/O55017/Q7TS72/Q6PHZ2/P26928/A3KGF7/F8VQL0/P68181/P29477/Q3UIZ8/Q02789/P35546/O54803/P31240/A0A0R4IZW4/Q64518/Q8R0X5/Q62035/Q6Q477/P30549/Q3KP20/P70227/B1B1A8/Q61616/Q61526/P61014/Q60930/A0A087WS83/Q9Z1M0/C8YIX4/Q8R3B1/P63094/Q8BSY0/P35375/B2RXC2/O09161/Q8CIH5/P97953/P15655/Q541T2/P21278/Q3UPA1/P26618/O09165/Q61125/P47937/P97772/P30677/P01139/P30558/Q3UR32/P63318/Q3UN66/P21803/E9QK53/Q91VB2/E9PZQ0/Q8K596/Q8VCR8/P35436/P11881/P32304/Q7TSI8/Q99J21/P97445	105
mmu05412	Arrhythmogenic right ventricular cardiomyopathy	46/2380	130/11633	5.19E-05	0.00188415	Q9Z1L5/Q01815/Q0PCR6/A2A864/Q924A0/E9QQ91/Q65CL1/Q8VHW3/Q9JJV4/Q62470/Q9Z1J1/A1A550/Q8CC27/Q02248/Q3TZS3/S4R2P9/Q99246/Q6PHS9/E9Q557/Q02789/Q64518/Q8R0X5/E9PXZ3/A0A0B4J1F0/Q62165/Q5RJF7/F8VPL1/O88602/Q3ZB20/O08532/Q14BH8/P82347/P19137/B8JK39/P11688/Q0VBD0/O70309/Q6PE70/Q8K596/Q61301/Q8R3Z5/A2A545/Q60675/P27782/Q3TYB0/Q8BGZ9	46
mmu00533	Glycosaminoglycan biosynthesis - keratan sulfate	13/2380	22/11633	8.16E-05	0.00266843	Q9EQC0/Q11204/Q9R1I1/A0A0R4J1C9/P54751/Q544T4/P15535/Q3U478/P97325/Q9CZ48/Q80WV3/Q9Z2Y2/Q9JJ04	13
mmu04072	Phospholipase D signaling pathway	72/2380	233/11633	9.52E-05	0.0028289	Q5SW28/O35083/A0A0R4J263/P39053/Q9QUI0/P97490/P20826/Q9D517/Q9QX11/Q9QVP9/Q3UDE9/Q62463/P20444/Q4VA93/Q8BMC3/Q925I7/P31938/Q3TMJ8/P01132/P39688/Q9JIW9/Q9R1C6/P32883/Q5J7N1/Q8VCC8/P84309/Q61469/A0A0A0MQ87/A3KGF7/P62331/Q3U0D7/Q9QYY0/O88673/D3YXJ0/Q8BZ98/P31240/A0A0R4IZW4/Q03385/D3YWQ0/P39054/E9PUQ8/Q5NCH9/Q68ED2/O08989/Q3TPX5/P47743/Q9JLN9/Q99JY8/Q68EF4/A0A140T8R6/P63094/Q9EQZ6/Q8CIH5/O70161/P63034/Q01341/F8VQ52/Q9WUA6/P27601/Q9D034/P26618/P97772/Q6NS52/P30558/Q61120/Q8K4X7/P62071/Q7TT21/O35904/Q91WG7/Q50L42/P35235	72
mmu04310	Wnt signaling pathway	76/2380	251/11633	0.00012846	0.00350054	P22726/P48455/Q9WVB2/Q3UN01/Q8BUN5/P56546/Q3UGL5/Q99MH6/Q924A0/E9QQ91/Q8C4U3/Q9QUI0/Q8K120/Q9Z1N6/Q923T9/Q80Z96/Q08122/P20444/Q4VA93/P11798/Q9Z1J1/A1A550/Q8BHJ5/O88572/A0A0R4J0A9/Q9WU66/A0A0R4J001/Q02248/P17553/Q6PHZ2/P97298/Q60591/Q80Y24/A7YQ68/A3KGF7/Q64527/P68181/O35468/Q2TBA6/Q62073/P60764/Q14A12/P30282/Q3TSW4/Q9WTX6/Q91Y86/Q8BQD1/P27467/Q549C9/Q9Z139/D3Z6Q6/P48755/Q3UMK5/Q3UVD5/Q91VN0/A2ARI4/O88712/F8VPR5/O35927/E9QKH8/Q61473/Q3ULA2/P63318/Q3UN66/O54908/Q9Z132/B1ASC1/Q3UN27/P97299/Q3UI35/O88566/Q8VE28/P63001/P27782/Q3TYB0/Q8BGZ9	76
mmu01521	EGFR tyrosine kinase inhibitor resistance	41/2380	119/11633	0.00025053	0.00630179	Q62120/P70424/P10417/P20444/Q4VA93/Q8BMC3/Q925I7/P31938/Q3TMJ8/P01132/Q04690/D3YZR2/P32883/Q5J7N1/P28028/Q8BSK8/A0A0A0MQ87/F8VQL0/Q9QYY0/P31240/A0A0R4IZW4/Q9WVH4/Q61526/Q9JLN9/Q61337/O54918/Q542N5/Q8CIH5/P15655/Q541T2/Q61592/Q9WUA6/P26618/Q3UTA9/Q61120/P63318/Q3UN66/P21803/E9QK53/O35904/Q7TSI8	41
mmu04725	Cholinergic synapse	53/2380	167/11633	0.00037097	0.00808725	Q9JMF3/Q5SW28/P32211/Q62120/Q01815/Q0PCR6/P97490/Q923T9/Q9JK97/P21836/Q543Z1/Q8BH52/Q9Z125/A0A0R4J082/Q61011/P10417/P20444/Q4VA93/P11798/P31938/Q3TMJ8/Q9ERZ4/P63250/P39688/P97414/Q99246/O55017/Q6PHZ2/Q8R4G9/P32883/Q5J7N1/P84309/A3KGF7/P68181/Q02789/P52187/P08752/Q61017/P70227/P48542/Q0VB45/P18872/Q01341/F8VQ52/Q9WUA6/P21278/Q3UPA1/P29387/P63318/Q3UN66/O35904/P11881/P97445	53

mmu04928	Parathyroid hormone synthesis, secretion and action	53/2380	167/11633	0.00037097	0.00808725	P28700/O09102/A0A0R4J021/E9Q394/Q9QUI0/P97490/Q8BH52/Q9Z125/A0A0R4J082/Q06219/Q3TYI4/P10417/P20444/Q4VA93/Q3UEI1/P31938/Q3TMJ8/Q8BWG8/O88572/A0A0R4J0A9/O35235/Q9R0S3/Q08775/P28028/P84309/Q01063/P48281/A3KGF7/Q68FM7/P68181/Q9DBP0/P08752/P70227/Q60929/Q61210/P63094/Q9D2V6/Q91VN0/Q01341/F8VQ52/P21278/Q3UPA1/Q9QY96/P27601/Q9D034/P70670/Q06186/Q5FW64/P63318/Q3UN66/Q64441/P11881/Q8CFN5	53
mmu04371	Apelin signaling pathway	61/2380	199/11633	0.00039893	0.00815304	Q9JMF3/Q5SW28/P12242/Q8BUN5/P09542/O70343/Q91WG5/Q9Z0J4/Q61982/P97490/O54950/Q3TWR3/Q8CGN5/P0DMC4/P16054/Q61011/Q6PAM0/P31938/Q3TMJ8/P0DP27/P0DP28/Q3UJF1/S4R2P9/Q60843/P32883/Q5J7N1/P84309/Q8BSK8/A3KGF7/P68181/P29477/Q3UIZ8/P11214/P08752/Q61017/P70227/Q60929/O08989/Q3TPX5/B1B1A8/P51667/Q9JLN9/P54310/Q01341/F8VQ52/Q9WUA6/P27601/Q9D034/Q9WU00/Q8C0T9/Q64729/P29387/Q9CQV6/P62071/E9PZQ0/Q8K596/Q8VCR8/P11881/Q61409/E9QLQ3/Q8CFN5	61
mmu05223	Non-small cell lung cancer	41/2380	122/11633	0.00045299	0.00871336	P28700/O08734/P42230/Q9JIA0/Q9JI11/P70424/P42232/P20444/Q4VA93/Q64261/P31938/Q3TMJ8/P01132/Q5EBH1/P51480/P22605/Q6DFX0/P32883/Q5J7N1/P28028/A0A0A0MQ87/F8VQL0/P35546/Q9WVH4/Q62137/A0A0R4J0R7/P22339/Q549C9/Q61337/P97793/Q8CIH5/O89106/Q9WUA6/Q61768/P28738/Q3UMY5/A0A3Q4EHV9/A7ISP9/P63318/Q3UN66/O35904	41
mmu04724	Glutamatergic synapse	53/2380	169/11633	0.0005111	0.00928489	Q9JMF3/P48455/Q8BMF5/Q01815/Q0PCR6/Q01098/Q3TXX4/P97490/P35438/Q03391/Q8BLE7/A0A0R4J0A6/P43006/Q3UYK6/Q9D415/Q61011/P20444/Q4VA93/Q9DCP2/P63250/P23818/Q7TNB5/Q99246/D3Z7P3/P84309/B1AS29/A3KGF7/P68181/P08752/D3YZU1/Q61017/P70227/Q5NCH9/Q68ED2/P47743/Q62108/P18872/Q68EF4/A0A140T8R6/P63094/Q80Z38/Q99MK8/Q01341/F8VQ52/P97772/P29387/P63318/Q3UN66/P35436/P11881/Q99JP6/Q50L42/P97445	53
mmu04722	Neurotrophin signaling pathway	56/2380	182/11633	0.00060978	0.01038057	Q3UFB7/Q8CE90/E9Q9B7/Q9QUI0/Q923T9/Q6PHU5/P15209/P18653/P10417/Q9WUI1/P11798/Q8BMC3/P31938/Q3TMJ8/Q9Z1E3/P0DP27/P0DP28/Q9WVS7/P21237/Q541P3/Q6PHZ2/P41242/P32883/Q5J7N1/P28028/A0A0A0MQ87/Q8K4B2/Q3UHC1/Q3UGX8/Q9QYY0/Q61144/Q3U4P5/O09039/P00520/Q9WVH4/O35099/Q9Z1B7/Q60778/Q91Y86/Q549C9/Q61337/Z4YK94/Q9JJP2/Q99PT1/Q9WUT3/Q8CIH5/Q9WUA6/P49138/Q3U2P8/P01139/Q61120/P28867/Q53YN4/O35904/P63001/P35235	56
mmu04024	cAMP signaling pathway	94/2380	338/11633	0.0006349	0.01038057	E1AZ71/Q91WA8/Q7TN16/Q01815/Q0PCR6/Q01098/P30873/Q543T0/Q60613/P22389/Q9QUI0/P97490/Q9EPL9/Q923T9/P35438/Q9R0K7/Q3UHH0/Q9Z239/Q03391/Q8BH52/Q9Z125/A0A0R4J082/Q8BWG9/P11798/Q3UEI1/P31938/Q3TMJ8/Q60992/Q7TSI6/Q9Z1E3/Q9ERZ4/P0DP27/P0DP28/Q61224/P23818/Q7TNB5/Q9EQX0/Q99246/P21237/Q541P3/Q6PHZ2/P57774/Q60829/P28028/Q8VCC8/P84309/Q01063/P68181/P70205/Q6NXJ9/Q02789/Q60612/P08752/P60764/Q14A12/Q64518/Q8R0X5/E9Q236/Q3UW12/Q6Q477/Q91Y86/Q61616/Q8CA95/P61014/Q61337/P63094/P54310/Q80T41/Q9EQZ6/Q0P543/P23204/Q542P9/F8VPR5/Q6P1D6/Q01341/F8VQ52/Q9WUA6/Q8C0T9/P30558/Q60748/Q3UQP0/Q61602/Q9R0C8/P62071/O35904/Q9JJZ8/P35436/P48787/Q497F1/P63001/Q61409/E9QLQ3/O35659/Q9EP66	94
mmu04720	Long-term potentiation	34/2380	99/11633	0.00086934	0.01327786	P48455/Q01815/Q0PCR6/Q01098/P97490/Q923T9/P35438/Q03391/P18653/P20444/Q4VA93/P11798/P31938/Q3TMJ8/Q9ERT9/P0DP27/P0DP28/P23818/Q7TNB5/Q6PHZ2/P32883/Q5J7N1/P28028/Q8VCC8/A3KGF7/P68181/P70227/Q9WUT3/F8VPR5/P97772/P63318/Q3UN66/P35436/P11881	34
mmu00562	Inositol phosphate metabolism	31/2380	88/11633	0.00089331	0.01327786	Q7TT16/E9QAN8/Q8CDA1/P17751/Q8K3R3/Q9EPW0/F6V2U0/Q3UEQ1/Q7TNC9/Q6P549/Q7TS72/E9Q7S0/Q8BYN3/A2AP18/A3KGF7/Q8BKC8/P59644/Q91WF7/Q8R3B1/Q6U7H8/B2RXC2/O70167/Q80XI4/Q8CIH5/O70161/Q9D2G5/Q9ES52/Q8CBQ5/Q9Z2L6/Q9JHU9/O35904	31
mmu04713	Circadian entrainment	47/2380	150/11633	0.00105152	0.0143293	Q9JMF3/Q01815/Q0PCR6/Q01098/Q9Z0J4/P97490/Q923T9/P35438/E9Q7P2/Q03391/Q61011/P20444/Q4VA93/P11798/O70361/P63250/P0DP27/P0DP28/P23818/Q7TNB5/Q99246/Q6PHZ2/P84309/A3KGF7/P68181/P70205/Q6NXJ9/P0C605/Q8BND1/P08752/Q61017/P70227/P48542/Q0VB45/P18872/P63094/O54943/A0A0R4J0U3/Q01341/F8VQ52/Q8C0T9/P29387/P63318/Q3UN66/E9PZQ0/P35436/P11881	47

mmu05034	Alcoholism	62/2380	210/11633	0.00105169	0.0143293	Q9JMF3/Q01098/Q60613/Q64478/P84228/Q64525/P35438/Q8VBY2/P15209/Q03391/Q8BH52/P62806/P24529/C0HKE9/P10853/Q9Z125/A0A0R4J082/Q61011/Q8BMC3/P31938/Q3TMJ8/Q64524/Q64522/P0DP27/P0DP28/Q3UJF1/P84244/P21237/Q541P3/P57774/Q60829/Q64523/P32883/Q5J7N1/P28028/P84309/A0A0A0MQ87/P68181/P08752/P0C0S6/Q61017/Q61616/C0HKE8/Q91WA3/P18872/P63094/Q6GSS7/Q99N13/A0A0R4J1F3/O35852/P13346/Q8CGP5/P68433/Q9JIM1/P29387/Q8CGP7/Q61120/Q8CCK0/Q6ZWY9/P35436/Q8CGP2/C0HKE7	62
mmu04510	Focal adhesion	84/2380	304/11633	0.00147578	0.01891567	P11087/O08863/A2CGA5/Q61711/A2A864/Q9EPC1/Q8BUR4/Q9QUI0/Q9ES46/P70424/E9Q2T3/Q64727/Q62523/P10417/P20444/Q4VA93/E9PYT0/Q8BMC3/Q62470/Q925I7/P31938/Q3TMJ8/Q71LX4/E9PUM4/Q8CDM9/Q61140/P01132/Q60992/Q7TSI6/P39688/Q7TPR4/Q02248/Q3TZS3/Q60841/P02463/O55222/P28028/A0A0A0MQ87/F8VQL0/Q3UHC1/Q3UGX8/Q3UIZ8/Q05895/A6H644/P31240/A0A0R4IZW4/P60764/Q14A12/P30282/Q3TSW4/Q80X90/B1B1A8/Q91Y86/P51667/Q91YM2/Q61292/E9PXZ3/Q62082/A0A0B4J1F0/Q61337/P27671/O70161/Q9QZR9/P97953/Q9WUA6/P26618/Q3UMT1/P19137/B8JK39/Q9R0C8/Q61120/P63318/Q3UN66/P11688/Q0VBD0/O08529/O70309/Q6PE70/Q8VCR8/O35904/Q60675/P63001/Q8BYI9/Q80YQ1	84
mmu04015	Rap1 signaling pathway	92/2380	338/11633	0.001504	0.01891567	Q0VG15/A2ALS5/O35608/Q6RHR9/Q03145/Q60613/Q9QUI0/P97490/G3X9J0/Q80TE4/P20826/Q9JJV2/P35438/E9Q0Y4/Q99NH2/A0A0R4J1Y4/P20444/Q4VA93/Q9WUI1/Q9WVQ1/Q925I7/P31938/Q3TMJ8/Q71LX4/E9PUM4/Q8CDM9/Q61140/P01132/Q60992/Q7TSI6/P52801/P0DP27/P0DP28/Q9JIW9/Q02248/Q5EBH1/P61148/Q6ZWS1/P32883/Q5J7N1/P28028/Q8VCC8/P84309/A3KGF7/F8VQL0/Q3UHC1/Q3UGX8/Q3UV74/Q8C0T5/P31240/A0A0R4IZW4/Q03385/P08752/P60764/Q14A12/P30999/O08989/Q3TPX5/Q9Z1B7/Q8BZ03/P18872/P63094/Q8C0Q9/Q9DAD6/Q9JK84/G5E8F1/Q9EQZ6/Q02858/P97953/P15655/Q541T2/Q6P1D6/Q01341/F8VQ52/Q9WUA6/P26618/P01139/P30558/Q8K1Y2/Q9R0C8/P63318/Q3UN66/P21803/E9QK53/O35904/P35436/Q9QUG9/P70429/P63001/O08543/Q7TSI8/Q80YQ1	92
mmu04270	Vascular smooth muscle contraction	61/2380	209/11633	0.00156268	0.01892578	P97718/Q8BUE5/E9QA16/Q01815/Q0PCR6/Q6URW6/Q08460/A0A286YD35/Q60613/P22389/Q9QUI0/P97490/Q62463/P16054/P20444/Q4VA93/Q9DBL0/P31938/Q3TMJ8/P0DP27/P0DP28/Q99246/P28028/P84309/A3KGF7/Q68FM7/P68181/Q3UIZ8/A6H644/Q02789/P0C605/Q8BND1/Q9WUP1/Q3UR44/G5E8V5/P70227/B1B1A8/Q61210/P63094/P63268/Q3UJ36/Q8VC81/P97391/Q6GTW1/Q01341/F8VQ52/P21278/Q3UPA1/P27601/Q9D034/Q9EPR2/Q3UMT1/P63318/Q3UN66/P28867/Q53YN4/Q61879/Q3UH59/Q8VCR8/P11881/Q50L42	61
mmu04921	Oxytocin signaling pathway	66/2380	230/11633	0.00165647	0.01934523	Q5SW28/P48455/Q05769/Q9Z1L5/Q01815/Q0PCR6/Q9QUI0/Q8K120/Q91WG5/P97490/O54950/Q3TWR3/Q923T9/Q8VHW3/P20444/Q4VA93/Q9JJV4/Q6PAM0/P11798/P31938/Q3TMJ8/P63250/P0DP27/P0DP28/Q8CC27/Q99246/Q9WVS7/Q6PHS9/Q6PHZ2/Q60591/P32883/Q5J7N1/P84309/A3KGF7/P68181/Q3UIZ8/A6H644/Q02789/P52187/P08752/P70227/B1B1A8/P48542/Q0VB45/P18872/P63094/Q5RJF7/F8VPL1/Q01341/F8VQ52/O88602/Q3ZB20/O08532/Q14BH8/Q9JHG6/Q3UMT1/P63318/Q3UN66/Q91VB2/E9PZQ0/Q8VCR8/Q8R3Z5/A2A545/P11881/Q50L42/Q8CFN5	66
mmu04810	Regulation of actin cytoskeleton	88/2380	323/11633	0.00182587	0.02058824	Q3UQ44/Q5DU57/E0CYU0/P32211/Q0VG15/Q6URW6/A2A864/Q76I79/Q8BUR4/Q9QUI0/Q9JJV2/Q5SQX6/Q9JKF1/Q64727/Q9WTL4/Q62470/Q925I7/P31938/Q3TMJ8/Q61140/Q8K1X4/P01132/Q60992/Q7TSI6/Q9ERZ4/Q7TPR4/Q3TZS3/P61148/Q6ZWS1/P26043/P32883/Q5J7N1/P28028/Q8K330/P45591/Q3UHW9/A0A0A0MQ87/Q3UIZ8/P26040/Q4KML7/A6H644/Q3UV74/Q5SW75/P31240/A0A0R4IZW4/P60764/Q14A12/O08989/Q3TPX5/B1B1A8/P51667/Q91YM2/E9PXZ3/Q62082/A0A0B4J1F0/Q61210/Q9DAD6/G5E8F1/Q80XI4/O70161/P15655/Q541T2/Q6P1D6/Q8BH43/P27601/Q9D034/P26618/Q61125/P30558/Q3UMT1/B8JK39/Q9R0C8/P11688/P21803/E9QK53/Q0VBD0/Q61879/Q3UH59/O70309/Q6PE70/P62071/O54785/P13020/Q8VCR8/O35904/P63001/Q91VR8/Q7TSI8	88

mmu04728	Dopaminergic synapse	58/2380	200/11633	0.00235795	0.0257016	Q9JMF3/P48455/Q01815/Q0PCR6/Q923T9/Q8BH52/P24529/Q9Z125/A0A0R4J082/Q61011/P20444/Q4VA93/Q9WUI1/P11798/Q8BWG8/Q9WTL8/P63250/P0DP27/P0DP28/P23818/Q7TNB5/Q60996/Q2NL51/Q99246/O55017/Q6PHZ2/B2RXC8/Q60829/P84309/A3KGF7/P68181/A1Y9I9/O08785/Q76MZ3/P08752/Q61017/P70227/Q9Z1B7/Q91Y86/Q61616/P48542/Q0VB45/P18872/P63094/P62715/Q9WUA6/Q7TNP2/Q61768/P28738/P30728/P29387/A2APX8/P63318/Q3UN66/P35436/P11881/Q6PD03/P97445	58
mmu05206	MicroRNAs in cancer	73/2380	263/11633	0.00256124	0.02701696	Q9R0G7/Q05769/O35516/O08734/Q9D3F7/Q9QUI0/Q61982/P31695/P70424/Q61823/P21447/E9Q2T3/P16054/O88898/P10417/P20444/Q4VA93/P58462/Q64261/P13864/P31938/Q3TMJ8/P61979/Q5FWJ5/Q9QXV8/P52801/Q61188/Q6AXH7/Q3UJF1/P51480/P27090/P17553/P26043/D3Z7P3/P32883/Q5J7N1/A0A0A0MQ87/F8VQL0/P26040/Q4KML7/P30306/Q3U535/Q9DBN8/P31240/A0A0R4IZW4/P00520/Q61526/P48754/Q9JLN9/Q09143/Q3UGD6/P27467/Q549C9/P58771/Q545Y3/O54918/Q542N5/Q8CIH5/F8VPR5/P26618/P06869/Q0V-BA8/P63318/Q3UN66/P11688/Q64441/P46414/O35904/Q1PSW8/O08543/Q8BYI9/Q7TSI8/Q80YQ1	73
mmu04911	Insulin secretion	41/2380	134/11633	0.00344146	0.03516747	O08786/Q01815/Q0PCR6/Q08460/A0A286YD35/O35526/Q497P1/P97490/Q923T9/Q8BH52/Q9Z125/A0A0R4J082/P20444/Q4VA93/P11798/Q99246/Q6PHZ2/P63011/Q0PD63/Q9EQZ7/P84309/Q7TN37/A3KGF7/P68181/P70205/Q6NXJ9/Q61743/Q02789/P70227/P63094/P09240/Q9EQZ6/P58391/Q9QYX7/Q01341/F8VQ52/P21278/Q3UPA1/P63318/Q3UN66/O35659	41
mmu04730	Long-term depression	31/2380	96/11633	0.00424655	0.04207943	Q9Z0J4/P20444/Q4VA93/P31938/Q3TMJ8/P23818/Q7TNB5/P32883/Q5J7N1/P28028/A3K-GF7/P0C605/Q8BND1/Q76MZ3/P08752/P70227/P18872/P63094/P62715/P21278/Q3UPA1/P27601/Q9D034/Q7TNP2/P97772/P63318/Q3UN66/E9PZQ0/P11881/Q50L42/P97445	31
mmu05210	Colorectal cancer	43/2380	144/11633	0.00456737	0.04392732	Q8BUN5/Q9JK91/O08734/Q924A0/E9QQ91/O70201/Q549P2/Q9QUI0/Q62312/P10417/P31938/Q3TMJ8/Q9Z1J1/A1A550/P01132/Q9JIW9/Q02248/P27090/Q8K3H0/P32883/Q5J7N1/P28028/Q8BSK8/A0A0A0MQ87/Q03385/P60764/Q14A12/Q91Y86/P22339/Q9JLN9/Q549C9/Q61337/O54918/Q542N5/Q56A15/Q9WUA6/Q64729/O35904/O88566/P63001/P27782/Q3TYB0/Q8BGZ9	43
mmu04912	GnRH signaling pathway	42/2380	141/11633	0.00526992	0.04923616	Q01815/Q0PCR6/Q8CE90/P97490/Q923T9/Q9QVP9/Q3UDE9/P20444/Q4VA93/Q9WUI1/P11798/P31938/Q3TMJ8/P0DP27/P0DP28/Q99246/Q6PHZ2/P32883/Q5J7N1/P84309/A0A0A0MQ87/A3KGF7/P68181/Q02789/P70227/Q9Z1B7/Q91Y86/P63094/P47809/Q543X6/Q01341/F8VQ52/P21278/Q3UPA1/Q06186/Q5FW64/P33434/Q3UG07/P28867/Q53YN4/P11881/Q50L42	42

Table S5. Significant gene sets in GO when using genes that are associated with any significant CpG sites in promoter region for the enrichment analysis

Ontology	ID	Description	GeneRatio	BgRatio	*P* value	FDR	geneID	Count
BP	GO:0032543	mitochondrial translation	21/2100	93/30636	9.95E-07	0.00255328	Mrps11/Yars2/Mrpl43/Alkbh1/Mrps14/Mrps14/Ndufa7/Gatb/Uqcc2/Mrpl57/Mrps21/Mrps21/Shmt2/Trmt10c/Tsfm/Mief1/Lars2/Mrps34/Mtg2/Mrpl2/Mrpl23	21
BP	GO:0050796	regulation of insulin secretion	48/2100	335/30636	1.04E-06	0.00255328	Rptor/Nnat/Nnat/Nnat/Nnat/Jak2/Mpc2/Gpr39/Uqcc2/Pde4c/Uts2/Sirt4/Ghrl/Stx4a/Kcnj11/Vsnl1/Epha5/Epha5/Nos1/Tardbp/Tardbp/Tardbp/Foxa2/Ano1/Ano1/Ano1/Phpt1/Bad/Bad/Per2/Per2/Adra2a/Tfap2b/Kcnq1/Kcnb1/Tcf7l2/Tcf7l2/Tcf7l2/Nr1d1/Srebf1/Alox5/Il1b/Pfkfb2/Pfkfb2/Pfkfb2/Pfkfb2/Pde3b/Pde3b	48
BP	GO:0140053	mitochondrial gene expression	27/2100	142/30636	1.18E-06	0.00255328	Mrps11/Yars2/Twnk/Mrpl43/Trmt5/Alkbh1/Mrps14/Mrps14/Mterf1a/Ndufa7/Chchd10/Gatb/Uqcc2/Mrpl57/Mrps21/Mrps21/Shmt2/Trmt10c/Tsfm/Mief1/Lars2/Foxo3/Mrps34/Mtg2/Mrpl2/Mettl4/Mrpl23	27
BP	GO:0071696	ectodermal placode development	12/2100	41/30636	1.27E-05	0.02048432	Pou2f1/Pou2f1/Pou2f1/Lrp6/Lrp6/Nrp1/Gnas/Gnas/Gnas/Ctnnb1/Gnas/Pou2f1	12
BP	GO:0071875	adrenergic receptor signaling pathway	14/2100	60/30636	4.19E-05	0.03670044	Adra1a/Adra1a/Akap13/Akap13/Adra1b/Gsk3a/Arrdc3/Nos1/Gnas/Gnas/Gnas/Adra2a/Kcnq1/Gnas	14
BP	GO:0060788	ectodermal placode formation	11/2100	40/30636	5.52E-05	0.03670044	Pou2f1/Pou2f1/Pou2f1/Lrp6/Lrp6/Gnas/Gnas/Gnas/Ctnnb1/Gnas/Pou2f1	11
BP	GO:0071697	ectodermal placode morphogenesis	11/2100	40/30636	5.52E-05	0.03670044	Pou2f1/Pou2f1/Pou2f1/Lrp6/Lrp6/Gnas/Gnas/Gnas/Ctnnb1/Gnas/Pou2f1	11
BP	GO:0014003	oligodendrocyte development	17/2100	85/30636	5.54E-05	0.03670044	Prdm8/Prdm8/Shh/Ulk4/Ulk4/Hdac11/Tenm4/Abca2/Tcf7l2/Tcf7l2/Tcf7l2/Eif2b5/Zfp488/Fgfr3/Fgfr3/Fgfr3/Fgfr3	17
BP	GO:0009743	response to carbohydrate	45/2100	358/30636	6.38E-05	0.03670044	Nnat/Nnat/Nnat/Nnat/Ccdc186/Mpc2/Gpr39/Pde4c/Sin3a/Ghrl/Rmi1/Pck2/Stx4a/Aqp4/Aqp4/Vsnl1/Epha5/Epha5/Mapk13/Foxa2/Ano1/Ano1/Ano1/Phpt1/Bad/Bad/Adra2a/Grk2/Grk2/Kcnb1/Tcf7l2/Tcf7l2/Tcf7l2/Nr1d1/Srebf1/Eif2b5/P2rx3/Il1b/Pfkfb2/Pfkfb2/Pfkfb2/Pfkfb2/Pde3b/Pde3b/Thbs1	45
BP	GO:0002089	lens morphogenesis in camera-type eye	13/2100	55/30636	6.78E-05	0.03670044	Hipk1/Pou2f1/Pou2f1/Pou2f1/Cryaa/Cryaa/Cryaa/Ctnnb1/Pou2f1/Fgfr3/Fgfr3/Fgfr3/Fgfr3	13
BP	GO:0030073	insulin secretion	50/2100	415/30636	7.73E-05	0.03670044	Rptor/Nnat/Nnat/Nnat/Nnat/Jak2/Cckar/Ccdc186/Mpc2/Gpr39/Uqcc2/Pde4c/Uts2/Sirt4/Ghrl/Stx4a/Kcnj11/Vsnl1/Epha5/Epha5/Nos1/Tardbp/Tardbp/Tardbp/Foxa2/Ano1/Ano1/Ano1/Phpt1/Bad/Bad/Per2/Per2/Adra2a/Tfap2b/Kcnq1/Kcnb1/Tcf7l2/Tcf7l2/Tcf7l2/Nr1d1/Srebf1/Alox5/Il1b/Pfkfb2/Pfkfb2/Pfkfb2/Pfkfb2/Pde3b/Pde3b	50
BP	GO:0090276	regulation of peptide hormone secretion	51/2100	426/30636	7.76E-05	0.03670044	Rptor/Nnat/Nnat/Nnat/Nnat/Jak2/Cckar/Mpc2/Gpr39/Uqcc2/Pde4c/Uts2/Rasl10b/Sirt4/Ghrl/Stx4a/Aimp1/Kcnj11/Vsnl1/Epha5/Epha5/Nos1/Tardbp/Tardbp/Tardbp/Foxa2/Ano1/Ano1/Ano1/Phpt1/Bad/Bad/Per2/Per2/Adra2a/Tfap2b/Kcnq1/Kcnb1/Tcf7l2/Tcf7l2/Tcf7l2/Nr1d1/Srebf1/Alox5/Il1b/Pfkfb2/Pfkfb2/Pfkfb2/Pfkfb2/Pde3b/Pde3b	51
BP	GO:0032024	positive regulation of insulin secretion	26/2100	168/30636	8.05E-05	0.03670044	Nnat/Nnat/Nnat/Nnat/Jak2/Mpc2/Gpr39/Ghrl/Stx4a/Vsnl1/Tardbp/Tardbp/Tardbp/Ano1/Ano1/Ano1/Phpt1/Bad/Bad/Tcf7l2/Tcf7l2/Tcf7l2/Pfkfb2/Pfkfb2/Pfkfb2/Pfkfb2	26
BP	GO:0009749	response to glucose	42/2100	330/30636	8.30E-05	0.03670044	Nnat/Nnat/Nnat/Nnat/Ccdc186/Mpc2/Gpr39/Pde4c/Sin3a/Ghrl/Rmi1/Pck2/Stx4a/Aqp4/Aqp4/Vsnl1/Epha5/Epha5/Foxa2/Ano1/Ano1/Ano1/Phpt1/Bad/Bad/Adra2a/Grk2/Grk2/Kcnb1/Tcf7l2/Tcf7l2/Tcf7l2/Nr1d1/Srebf1/Eif2b5/Pfkfb2/Pfkfb2/Pfkfb2/Pfkfb2/Pde3b/Pde3b/Thbs1	42
BP	GO:0071880	adenylate cyclase-activating adrenergic receptor signaling pathway	12/2100	49/30636	8.86E-05	0.03670044	Adra1a/Adra1a/Akap13/Akap13/Adra1b/Arrdc3/Nos1/Gnas/Gnas/Gnas/Adra2a/Gnas	12

BP	G0:0006884	cell volume homeostasis	16/2100	80/30636	9.08E-05	0.03670044	Slc12a7/Aqp11/Cln3/Cln3/Aqp4/Aqp4/Slc12a8/Ano6/Sctr/Sctr/Clcn3/Clcn3/Clcn3/Add1/Add1/Add1	16
BP	G0:0009746	response to hexose	42/2100	333/30636	0.00010185	0.03765758	Nnat/Nnat/Nnat/Nnat/Ccdc186/Mpc2/Gpr39/Pde4c/Sin3a/Ghrl/Rmi1/Pck2/Stx4a/Aqp4/Aqp4/Vsnl1/Epha5/Epha5/Foxa2/Ano1/Ano1/Ano1/Phpt1/Bad/Bad/Adra2a/Grk2/Grk2/Kcnb1/Tcf7l2/Tcf7l2/Tcf7l2/Nr1d1/Srebf1/Eif2b5/Pfkfb2/Pfkfb2/Pfkfb2/Pfkfb2/Pde3b/Pde3b/Thbs1	42
BP	G0:0033131	regulation of glucokinase activity	7/2100	18/30636	0.00011419	0.03765758	Foxa2/Bad/Bad/Pfkfb2/Pfkfb2/Pfkfb2/Pfkfb2	7
BP	G0:0033133	positive regulation of glucokinase activity	6/2100	13/30636	0.00011607	0.03765758	Bad/Bad/Pfkfb2/Pfkfb2/Pfkfb2/Pfkfb2	6
BP	G0:0034284	response to monosaccharide	42/2100	335/30636	0.00011644	0.03765758	Nnat/Nnat/Nnat/Nnat/Ccdc186/Mpc2/Gpr39/Pde4c/Sin3a/Ghrl/Rmi1/Pck2/Stx4a/Aqp4/Aqp4/Vsnl1/Epha5/Epha5/Foxa2/Ano1/Ano1/Ano1/Phpt1/Bad/Bad/Adra2a/Grk2/Grk2/Kcnb1/Tcf7l2/Tcf7l2/Tcf7l2/Nr1d1/Srebf1/Eif2b5/Pfkfb2/Pfkfb2/Pfkfb2/Pfkfb2/Pde3b/Pde3b/Thbs1	42
BP	G0:0016579	protein deubiquitination	26/2100	173/30636	0.00013183	0.04060335	Usp10/Usp7/Usp7/Otud4/Otud4/Usp31/Sart3/Otud7a/Shmt2/Usp29/Usp29/Usp48/Usp48/Usp2/Otud6b/Otud6b/Usp19/Usp19/Usp19/Usp19/Atxn3/Atxn3/Atxn3/Mindy1/Otub2/Yod1	26
BP	G0:0048384	retinoic acid receptor signaling pathway	14/2100	67/30636	0.00015055	0.0442625	Rarg/Tgif1/Tgif1/Cnot1/Cnot1/Cnot1/Klf2/Ctbp2/Rxra/Rxra/Esrrg/Rara/Rara/Zfp536	14
BP	G0:0006333	chromatin assembly or disassembly	28/2100	195/30636	0.0001651	0.0464301	Nap1l5/H2bc9/H2bc18/H2bc7/Hira/H2bc21/Smarcc2/Smarcc2/Sart3/H3f3a/Oip5/Rrp8/Chd3/Chd3/H4c8/Spty2d1/Naa60/Naa60/Naa60/H3c8/Suv39h2/Suv39h2/Noc2l/Smarca5/Smarcd2/H2bc4/H2bc22/Brd2	28
BP	G0:0002791	regulation of peptide secretion	51/2100	440/30636	0.00017408	0.04658265	Rptor/Nnat/Nnat/Nnat/Nnat/Jak2/Cckar/Mpc2/Gpr39/Uqcc2/Pde4c/Uts2/Rasl10b/Sirt4/Ghrl/Stx4a/Aimp1/Kcnj11/Vsnl1/Epha5/Epha5/Nos1/Tardbp/Tardbp/Tardbp/Foxa2/Ano1/Ano1/Ano1/Phpt1/Bad/Bad/Per2/Per2/Adra2a/Tfap2b/Kcnq1/Kcnb1/Tcf7l2/Tcf7l2/Tcf7l2/Nr1d1/Srebf1/Alox5/Il1b/Pfkfb2/Pfkfb2/Pfkfb2/Pfkfb2/Pde3b/Pde3b	51
BP	G0:0006334	nucleosome assembly	19/2100	111/30636	0.00018739	0.04658265	Nap1l5/H2bc9/H2bc18/H2bc7/Hira/H2bc21/Sart3/H3f3a/Oip5/H4c8/Spty2d1/Naa60/Naa60/Naa60/H3c8/Smarca5/H2bc4/H2bc22/Brd2	19
BP	G0:1903391	regulation of adherens junction organization	6/2100	14/30636	0.00019132	0.04658265	Rdx/Rdx/Ptpn23/Add1/Add1/Add1	6
BP	G0:0090087	regulation of peptide transport	51/2100	442/30636	0.00019445	0.04658265	Rptor/Nnat/Nnat/Nnat/Nnat/Jak2/Cckar/Mpc2/Gpr39/Uqcc2/Pde4c/Uts2/Rasl10b/Sirt4/Ghrl/Stx4a/Aimp1/Kcnj11/Vsnl1/Epha5/Epha5/Nos1/Tardbp/Tardbp/Tardbp/Foxa2/Ano1/Ano1/Ano1/Phpt1/Bad/Bad/Per2/Per2/Adra2a/Tfap2b/Kcnq1/Kcnb1/Tcf7l2/Tcf7l2/Tcf7l2/Nr1d1/Srebf1/Alox5/Il1b/Pfkfb2/Pfkfb2/Pfkfb2/Pfkfb2/Pde3b/Pde3b	51
BP	G0:1903322	positive regulation of protein modification by small protein conjugation or removal	32/2100	238/30636	0.000205	0.04735421	Birc3/Birc3/Pttg1ip/Pef1/Klhl40/Smad7/Sart3/Gsk3a/Dcun1d3/Arrdc3/Mta1/Mta1/Rasd2/Ubb/Commd1/Kdm1a/Kdm1a/Dcun1d5/Pdcd6/Brca1/Rnf180/Traf7/Traf7/Dcun1d1/Dcun1d1/Pias1/Pias1/Ctr9/Fgfr3/Fgfr3/Fgfr3/Fgfr3	32
CC	G0:0000313	organellar ribosome	22/2120	112/31010	6.21E-06	0.00235933	Mrps11/Mrpl43/Mrps14/Mrps14/Ndufa7/Mrpl40/Mrpl30/Mrpl14/Mrpl57/Mrpl32/Mrps21/Mrps21/Mrpl50/Mief1/Mrps34/Mrpl45/Mtg2/Mrpl48/Mrpl48/Mrpl2/Dap3/Mrpl23	22
CC	G0:0005761	mitochondrial ribosome	22/2120	112/31010	6.21E-06	0.00235933	Mrps11/Mrpl43/Mrps14/Mrps14/Ndufa7/Mrpl40/Mrpl30/Mrpl14/Mrpl57/Mrpl32/Mrps21/Mrps21/Mrpl50/Mief1/Mrps34/Mrpl45/Mtg2/Mrpl48/Mrpl48/Mrpl2/Dap3/Mrpl23	22

CC	GO:0005814	centriole	31/2120	207/31010	3.21E-05	0.00725808	Hyls1/Cetn4/Top2a/Bnip2/Bnip2/Ccp110/Mdm1/Mdm1/Mdm1/Mdm1/Ccsap/Hspa1a/Cep76/Odf2/Wdr90/Hap1/Sdccag8/Cep170/Cep170/Kif3a/Sclt1/Gle1/Alms1/Alms1/Saxo2/Akna/Tsks/Fam161a/Ccdc78/Cchcr1/Cchcr1	31
CC	GO:0005759	mitochondrial matrix	49/2120	394/31010	3.82E-05	0.00725808	Mrps11/Twnk/Mrpl43/Hadha/Hadhb/Trmt5/Mrps14/Mrps14/Mterf1a/Ndufa7/Prdx1/Uqcc2/Mrpl40/Mrpl30/Acot11/Acsm2/Sirt4/Mrpl14/Mrpl57/Mrpl32/Mrps21/Mrps21/Shmt2/Mrpl50/Trmt10c/Tsfm/Mief1/Pde12/Acss3/Foxo3/Brca1/Mrps34/Acot13/Atxn3/Atxn3/Atxn3/Mrpl45/Mtg2/Mrpl48/Mrpl48/Polg/Mrpl2/Iscu/Mettl4/Dhx30/Dap3/Snca/Acat1/Mrpl23	49
CC	GO:0070369	beta-catenin-TCF7L2 complex	7/2120	17/31010	7.29E-05	0.01086509	Tcf4/Tcf4/Ctnnb1/Tcf7l2/Tcf7l2/Tcf7l2/Tcf4	7
CC	GO:0071664	catenin-TCF7L2 complex	7/2120	18/31010	0.0001123	0.01086509	Tcf4/Tcf4/Ctnnb1/Tcf7l2/Tcf7l2/Tcf7l2/Tcf4	7
CC	GO:0060199	clathrin-sculpted glutamate transport vesicle	6/2120	13/31010	0.00011437	0.01086509	Otof/Otof/Otof/Dnajc5/Rab3a/Rab3a	6
CC	GO:0060203	clathrin-sculpted glutamate transport vesicle membrane	6/2120	13/31010	0.00011437	0.01086509	Otof/Otof/Otof/Dnajc5/Rab3a/Rab3a	6
CC	GO:0005840	ribosome	43/2120	352/31010	0.00016479	0.0126405	Mrps11/Mrpl43/Mrps14/Mrps14/Ndufa7/Rpl12/Rpl12/Mrpl40/Mrpl30/Larp4b/Mrpl14/Mrpl57/Mrpl32/Mrps21/Mrps21/Rps13/Rps13/Fau/Fau/Rpl6/Rpl6/Mrpl50/Rps15/Rps15/Mief1/Mrps34/Mrpl45/Mtg2/Rps14/Mrpl48/Mrpl48/Mrpl2/Rpl30/Rpl30/Nufip2/Dap3/Elavl4/Elavl4/Snca/Mcts2/Rpl15/Mrpl23/Uba52	43
CC	GO:0042581	specific granule	8/2120	25/31010	0.00017755	0.0126405	Adam8/Adam8/Adam8/Vamp1/Stx4a/Clcn3/Clcn3/Clcn3	8
CC	GO:0044391	ribosomal subunit	36/2120	279/31010	0.00018662	0.0126405	Mrps11/Mrpl43/Mrps14/Mrps14/Rpl12/Rpl12/Mrpl40/Mrpl30/Mrpl14/Mrpl57/Mrpl32/Mrps21/Mrps21/Rps13/Rps13/Fau/Fau/Rpl6/Rpl6/Mrpl50/Rps15/Rps15/Mief1/Mrps34/Mrpl45/Rps14/Mrpl48/Mrpl48/Mrpl2/Rpl30/Rpl30/Dap3/Mcts2/Rpl15/Mrpl23/Uba52	36
CC	GO:0001650	fibrillar center	31/2120	228/31010	0.00019959	0.0126405	Cilk1/Uso1/Rnmt/Gar1/Smug1/Mri1/Smad7/Malt1/Nrip1/Acaca/Fblim1/Ncl/Ip6k1/Nuak1/Cc2d1a/Rpain/Rpain/Rpain/Rpain/Akna/Wdr33/Wdr33/Wdr33/Mtdh/Nufip1/Exosc8/Smarca5/Cd2bp2/Mrpl23/Mbd6/Mbd6	31
CC	GO:0000315	organellar large ribosomal subunit	13/2120	68/31010	0.0006211	0.03371695	Mrpl43/Mrpl40/Mrpl30/Mrpl14/Mrpl57/Mrpl32/Mrpl50/Mief1/Mrpl45/Mrpl48/Mrpl48/Mrpl2/Mrpl23	13
CC	GO:0005762	mitochondrial large ribosomal subunit	13/2120	68/31010	0.0006211	0.03371695	Mrpl43/Mrpl40/Mrpl30/Mrpl14/Mrpl57/Mrpl32/Mrpl50/Mief1/Mrpl45/Mrpl48/Mrpl48/Mrpl2/Mrpl23	13
CC	GO:0060198	clathrin-sculpted vesicle	6/2120	18/31010	0.00091898	0.04656152	Otof/Otof/Otof/Dnajc5/Rab3a/Rab3a	6
MF	GO:0047696	beta-adrenergic receptor kinase activity	7/2082	12/30629	3.88E-06	0.00490966	Grk2/Grk2/Grk6/Grk6/Grk6/Grk6/Grk6	7
MF	GO:1990380	Lys48-specific deubiquitinase activity	11/2082	34/30629	9.24E-06	0.00584814	Usp7/Usp7/Usp19/Usp19/Usp19/Usp19/Atxn3/Atxn3/Atxn3/Mindy1/Yod1	11
MF	GO:0004703	G protein-coupled receptor kinase activity	7/2082	16/30629	4.39E-05	0.01215592	Grk2/Grk2/Grk6/Grk6/Grk6/Grk6/Grk6	7
MF	GO:0004843	thiol-dependent deubiquitinase	24/2082	148/30629	6.17E-05	0.01215592	Usp10/Usp7/Usp7/Otud4/Otud4/Usp31/Otud7a/Usp29/Usp29/Usp48/Usp48/Usp2/Otud6b/Otud6b/Usp19/Usp19/Usp19/Usp19/Atxn3/Atxn3/Atxn3/Mindy1/Otub2/Yod1	24

MF	G0:0047391	alkylglycerophos-phoethanolamine phosphodiesterase activity	8/2082	12/30629	6.33E-05	0.01215592	Gnas/Gnas/Gnas/Gna11/Gna11/Gnas	6
MF	G0:0008242	omega peptidase activity	25/2082	158/30629	6.64E-05	0.01215592	Usp10/Usp7/Usp7/Otud4/Otud4/Usp31/Otud7a/Usp29/Usp29/Usp48/Usp48/Usp2/Otud6b/Otud6b/Ggt7/Usp19/Usp19/Usp19/Usp19/Atxn3/Atxn3/Atxn3/Mindy1/Otub2/Yod1	25
MF	G0:0035254	glutamate receptor binding	22/2082	131/30629	7.20E-05	0.01215592	Adora2a/Cabp1/Cabp1/Prnp/Prnp/Calm1/Calm1/Shank1/Gnas/Gnas/Gnas/Gria1/Gria1/Ctnnb1/Camk2a/Camk2a/Dlg4/Gnas/Il1r1/Il1r1/Grin2a/Homer3	22
MF	G0:0101005	deubiquitinase activity	24/2082	150/30629	7.68E-05	0.01215592	Usp10/Usp7/Usp7/Otud4/Otud4/Usp31/Otud7a/Usp29/Usp29/Usp48/Usp48/Usp2/Otud6b/Otud6b/Usp19/Usp19/Usp19/Usp19/Atxn3/Atxn3/Atxn3/Mindy1/Otub2/Yod1	24
MF	G0:0035256	G protein-coupled glutamate receptor binding	6/2082	24/30629	0.00012335	0.01735095	Adora2a/Cabp1/Cabp1/Prnp/Prnp/Calm1/Calm1/Homer3	8
MF	G0:0019783	ubiquitin-like protein-specific protease activity	26/2082	176/30629	0.00015333	0.01924642	Usp10/Usp7/Usp7/Otud4/Otud4/Usp31/Otud7a/Usp29/Usp29/Usp48/Usp48/Usp2/Otud6b/Otud6b/Usp19/Usp19/Usp19/Usp19/Atxn3/Atxn3/Atxn3/Mindy1/Otub2/Yod1/Senp8/Senp8	26
MF	G0:0031681	G-protein beta-subunit binding	10/2082	38/30629	0.00016723	0.01924642	Gng13/Rasd2/Rgs7/Gnas/Gnas/Gnas/Gria1/Gria1/Gngt2/Gnas	10
MF	G0:0010851	cyclase regulator activity	7/2082	20/30629	0.0002338	0.02466558	Guca1b/Calm1/Calm1/Gnas/Gnas/Gnas/Gnas	7
MF	G0:0031208	POZ domain binding	5/2082	10/30629	0.00027246	0.02653348	Zbtb21/Zbtb21/Zbtb21/Zbtb21/Klhl17	5
MF	G0:0031628	opioid receptor binding	7/2082	21/30629	0.00033018	0.029858	Penk/Gnas/Gnas/Gnas/Grk2/Grk2/Gnas	7
MF	G0:0072542	protein phosphatase activator activity	6/2082	16/30629	0.00043278	0.03652676	Calm1/Calm1/Ptpa/Ptpa/Ppp2r5c/Ppp2r5a	6
MF	G0:0031698	beta-2 adrenergic receptor binding	7/2082	23/30629	0.00061721	0.04434476	Gnas/Gnas/Gnas/Gria1/Gria1/Dlg4/Gnas	7
MF	G0:0042171	lysophosphatidic acid acyltransferase activity	7/2082	23/30629	0.00061721	0.04434476	Agpat1/Agpat3/Abhd4/Abhd4/Pnpla3/Pnpla3/Agpat1	7
MF	G0:0001093	TFIIB-class transcription factor binding	6/2082	17/30629	0.00063049	0.04434476	Tbp/Tcf4/Tcf4/Crebbp/Crebbp/Tcf4	6
MF	G0:0003735	structural constituent of ribosome	30/2082	236/30629	0.00071536	0.04766526	Mrps11/Mrpl43/Mrps14/Mrps14/Ndufa7/Rpl12/Rpl12/Mrpl30/Mrpl14/Mrpl57/Mrpl32/Mrps21/Mrps21/Rps13/Rps13/Fau/Fau/Rpl6/Rpl6/Rps15/Rps15/Mrps34/Rps14/Mrpl2/Rpl30/Rpl30/Dap3/Rpl15/Mrpl23/Uba52	30